Mon. Not. R. Astron. Soc. **288,** 431–456 (1997)

The nature of the silicon carbide in carbon star outflows

A. K. Speck,[1] M. J. Barlow[1] and C. J. Skinner[2]

[1]*Department of Physics and Astronomy, University College London, Gower Street, London WC1E 6BT*
[2]*Space Telescope Science Institute, 3700 San Martin Drive, Baltimore, MD 21218, USA*

Accepted 1997 February 19. Received 1997 February 17; in original form 1996 December 30

ABSTRACT

We present 7.5–13.5 μm UKIRT CGS3 spectra of 32 definite or candidate carbon stars. In addition to the extreme carbon star AFGL 3068, the only carbon star previously known to show the 11-μm silicon carbide (SiC) feature in absorption, we have discovered three further examples of sources that show SiC in net absorption, namely IRAS 02408+5458, AFGL 2477 and AFGL 5625. We investigate the mineralogy of carbon star SiC and its relationship to meteoritic dust by using a χ^2-minimization routine to fit the observed SiC features, and laboratory optical constants that have been published for a variety of SiC samples. With the exception of R For, all of the observed SiC features are best fitted by α-SiC grains. Excluding V414 Per, all of the sources with 8–13 μm colour temperatures >1200 K (corresponding to mass-loss rates at the bottom end of the range) are best fitted by α-SiC in pure emission, whereas all but one of the sources with 8–13 μm colour temperatures <1200 K (corresponding to higher mass-loss rates) are best fitted using self-absorbed α-SiC emission. The four sources whose SiC features are in net absorption (and which have the lowest 8–13 μm colour temperatures and therefore presumably the highest mass-loss rates) are also well fitted by self-absorbed α-SiC emission, but with higher optical depths. Given that β-SiC is the form most commonly found in meteorites, we have searched for evidence of β-SiC in the circumstellar shells of all these carbon stars. However, our observations provide no unambiguous evidence for the presence of β-SiC around these stars, with all of the observed SiC features being best explained in terms of α-SiC grains. The self-absorption that we find in the observed SiC emission features has not previously been taken into account in radiative transfer modelling, and so the amount of SiC present in the outflows has probably been underestimated in the past.

Key words: stars: carbon – circumstellar matter – dust, extinction – infrared: stars.

1 INTRODUCTION

It has been known for more than two decades that dust particles form in the atmospheres of cool stars and are ejected into the interstellar medium (ISM); cf. Gilra (1971), Woolf (1973), Stephens (1980), Mathis (1990) and Evans (1994). In this context there has been a great deal of work published on silicon carbide (SiC). From equilibrium condensation models, Friedemann (1969) and Gilman (1969) showed that SiC should condense in the atmospheres of carbon stars. Following the work of Gilra & Code (1971), Hackwell (1972) and Treffers & Cohen (1974), a broad infrared emission feature seen in the spectra of many carbon stars, peaking between about 11.0 and 12.5 μm, has been attributed to solid SiC particles. SiC is therefore believed to be a significant constituent of the dust around carbon stars. There are, in fact, about 70 different forms of SiC, known as polytypes, and a large number of papers have been published discussing which form most closely fits the observed feature near 11 μm. All these polytypes are variants of the same basic structure, based on a tetrahedral group of silicon and carbon atoms (Taylor & Jones 1960). These 70 different forms of SiC can be divided into two basic groups: α-SiC and β-SiC. The α-SiC form has a hexagonal or rhombohedric crystal structure, and is very stable up to approximately 2700° C. The β-SiC form has a cubic

structure and, whilst also very stable, is in general slightly less thermodynamically favoured than α-SiC. β-SiC is the favoured type when condensation takes place in a vacuum. β-SiC will transform into α-SiC at temperatures above about 2100° C, but it is thermodynamically unlikely that this process will work in reverse. Very little (a few per cent at best) α-SiC will transform into β-SiC (I. P. Parkin, private communication). The difference between these two forms is small, both structurally and thermodynamically (below 2100° C), but they can be distinguished by crystallographic techniques and by their infrared spectra. One of the aims of the current work was to determine whether either type predominates in the circumstellar outflows around carbon stars, via observations of the 11-μm spectra of a significant sample of carbon stars.

2 BACKGROUND

2.1 α-SiC versus β-SiC in astronomical environments

In the literature concerning the 11-μm SiC feature in carbon star spectra, much of the work already published is somewhat contradictory, and certainly needs some introduction. In order to address this problem, we therefore begin with a review of some of the existing work on this topic.

Gilman (1969) and Friedemann (1969) predicted that SiC could condense in the atmospheres of cool carbon stars. Gilra & Code (1971) used this information, together with calculations published by Gilra (1972), to predict that SiC should re-emit absorbed radiation as a feature in the 10–13 μm region. Hackwell (1972) found an emission feature in two carbon stars in this spectral region that was quite similar to Gilra's calculated emission feature. Treffers & Cohen (1974) published high-resolution spectra of the SiC feature in several carbon stars, and made use of unpublished calculations by Gilra, based on α-SiC optical constants, to interpret these spectra. It was shown that small particles of a single shape produce several narrow emission features situated between the longitudinal and transverse vibrational wavelengths of α-SiC at 10.2 and 12.8 μm, and that particles of different shapes would produce features at different wavelengths between these limits (see also Kozasa et al. 1996). It was also shown that a continuous distribution of shapes should give a smooth feature with cut-on and cut-off wavelengths corresponding to the longitudinal and transverse vibrational modes of SiC.

Stephens (1980) investigated various dust species (silicates, carbon and SiC) with a view to explaining the visible and ultraviolet extinction in the ISM. He chose to use β-SiC for his experiments, as it is the most stable structural form of SiC below about 2000 K. He found that in order to fit the interstellar extinction curve, the SiC particles needed to be very much smaller (radius < 0.005 μm) than the particles he used to produce spectra. He also used the fact that no 11.5-μm SiC feature is seen in the extinction curve of the ISM to constrain the SiC abundance. He concluded that 'SiC is probably not the major contributor to the observed visible and ultraviolet extinction', contradicting the conclusion of Gilra (1971) that SiC was one of the constituents needed to explain the entire extinction curve of the ISM.

Whittet, Duley & Martin (1990) also investigated the presence of SiC in the ISM. They concurred with Stephens (1980) that SiC is not a major contributor to the ISM extinction curve, estimating that less than 5 per cent of Si atoms in the ISM can reside in SiC dust. To reconcile this lack of interstellar SiC with the fact that SiC is found in the circumstellar shells of carbon stars, they suggested that SiC is rare in carbon stars, citing the lack of SiC absorption in stars with optically thick circumstellar shells as evidence. However, as will be seen in Section 7, SiC has now been seen in absorption in the spectra of several carbon stars. Another solution they suggested is that SiC may be subject to selective grain destruction in the ISM, and that this could also explain the rarity of SiC found in meteorites.

Several papers have used laboratory analyses of SiC samples to simulate the SiC emission feature at 11–13 μm, with a view to identifying observed astronomical features. Friedemann et al. (1981) used two forms of commercially available α-SiC. They used five samples with various size distributions, made up of measured mixtures of the two types of α-SiC. They found that the bandwidth of the absorption feature was not affected by the size distribution or by impurities, but that the absorption peak (i.e., where the ratio of the recorded intensity to the continuum intensity reaches a minimum) was affected, so that when comparing different grain-size distributions, the larger grain sizes give rise to reduced absorption peaks. They found a peak wavelength of 11.8 μm before correcting for their experimental substrate, and a wavelength peak of 11.4 μm after correction. They also fitted one of their sample spectra to the spectrum of Y CVn. Goebel, Cheeseman & Gerbault (1995) describe the unusual J-type carbon star Y CVn as having a 'somewhat different SiC band profile than normally found in other visible carbon stars'. However, our CGS3 spectrum of Y CVn is not particularly unusual in the shape and peak wavelength of its SiC feature (see Fig. 3 and Table 2 below).

Borghesi et al. (1985) performed a comparative laboratory study of several samples of both α-SiC and β-SiC. Their samples were ground and sedimented to various degrees in order to determine the effects of the size distribution. They found the feature to peak in wavelength at about 11.8 μm for α-SiC, and at about 11.4 μm for β-SiC, before correction for their experimental technique, and at 11.4 and 11.0 μm after correction. This agrees well with the results of Friedemann et al. (1981). Borghesi et al. also found that, for their less pure α-SiC samples (i.e., 89 per cent SiC rather than 99 per cent SiC, with carbon, silicon, metallic iron and SiO_2 impurities), the peak wavelength shifted towards longer wavelengths as the particle size increased. This did not occur for their purest α-SiC, nor for their β-SiC samples. Comparing this with the results of Friedemann et al. (1981), there are some obvious discrepancies as Friedemann et al. found no changes in the emission feature due to impurities.

Pégourié (1988) set out to derive a synthetic dielectric function for SiC, from which spectral features could be predicted. He argued that the work of Baron et al. (1987) showed α-SiC to be the best candidate to reproduce the 11–11.5 μm feature in the *IRAS* Low Resolution Spectrometer (LRS) spectra of carbon stars. However, what Baron et al. actually concluded was that 'the shape of the strongest feature is quite similar to the mass absorption of α-SiC'. Taken together with their statement that 'the feature

becomes stronger and narrower as the temperature of the underlying continuum increases', this implies that α-SiC probably gives a good fit to features in the spectra of the carbon stars with the most optically thin dust shells. However, the same conclusion might not necessarily be applicable to cooler stars and to features produced by optically thick shells. Having decided to use α-SiC, Pégourié (1988) derived a comprehensive dielectric function by compiling partial data from a number of different authors and using a Kramers–Kronig analysis. He found that slight changes in impurities or morphology have a huge impact on the shape of the feature. This is consistent with the findings of Borghesi et al. (1985) and contradicts the work of Friedemann et al. (1981) discussed above. This conclusion that morphology has a big influence is also consistent with the work of Gilra (1973), presented by Treffers & Cohen (1974), regarding the sensitivity of the feature wavelength to particle shape for single-shape particles. Pégourié (1988) found that the 'synthetic' α-SiC feature he had created had a peak wavelength of 11.33 ± 0.5 μm. This is quite similar to the results of both Friedemann et al. (1981) and Borghesi et al. (1985).

2.2 Silicon carbide in meteorites

Goebel et al. (1995) also described work done on SiC inclusions found in meteorites. The fact that SiC is found in meteorites implies that it was present in the solar nebula and presumably originated around carbon stars. Goebel et al. (1995) note that nearly all the SiC inclusions found in meteorites are of the β-SiC form. Hoppe et al. (1994) found SiC grains in the Murchison meteorite. Under a scanning electron microscope the grains appeared at first to be hexagonal (α-SiC is hexagonal). However, when analysed using Raman spectroscopy over the 9.5–16.7 μm wavelength range (Virag et al. 1992), the spectrum revealed the particles to be β-SiC.

Since the work reviewed above has suggested α-SiC to be the main form of SiC around carbon stars, it seems prudent at this point to discuss some of the work published on meteoritic SiC in more detail.

The first unambiguous identification of SiC in meteorites was by Bernatowicz et al. (1987). The SiC found was of the β-SiC form, and the crystal grains were 0.1–1 μm in size. Bernatowicz et al. (1987) concluded that the SiC was probably formed in the atmospheres of late-type, carbon-rich stars. Since then, the main aim of papers on meteoritic SiC seems to have been to establish what sources are responsible for the SiC found. There has also been some discussion of the grain sizes and of the abundance (or lack) of SiC. Studies of the isotopic composition of SiC, including nitrogen and noble gases trapped during crystallization, have been performed, and the compositions compared to theoretical compositions for various stellar sources. Isotopic compositions on the Earth are basically uniform, so deviations from terrestrial compositions are taken to be evidence of a pre-solar origin.

Tang et al. (1989) looked at SiC found in carbonaceous chondrites. They found single grains up to 12 μm in diameter. This is much larger than the grain sizes predicted by circumstellar grain condensation models (e.g. Kozasa et al. 1996) or by radiative transfer fits to the overall energy distribution (e.g. Griffin 1990). Tang et al. found that most of the carbon and nitrogen isotope ratios were indicative of nucleosynthetic processes believed to occur in carbon-rich AGB stars, whilst a few indicated possible nova sources. Based on this and the silicon isotopic composition, they concluded that the meteoritic SiC in their sample came from at least four separate types of stars, including a nova. They also pointed out the surprising rarity of SiC in meteorites. Carbon stars are thought to contribute approximately 1/3 of the total mass ejected into the ISM by stars (Tielens 1990), and yet even primitive chondrites contain only 0.004 per cent of their silicon in SiC (the rest being in the form of silicates). To address this problem, Tang et al. suggested some destruction processes. (a) Supernova shocks – they ruled out these on the grounds that microdiamonds in the solar nebula would also be affected, and that there is no evidence of this. (2) Selective interstellar processes – given that SiC has not been seen in the ISM, they suggested that there is a rapid destruction mechanism at work on SiC. However, they argued that in order to deplete the SiC by the required amount to fit the observations, the SiC should have a lifetime in the ISM of only 10^5 yr, which is much less than the apparent cosmic ray exposure age of 10 Myr of meteoritic SiC grains. Given that SiC is a very unreactive material and as such is used for lining fusion reactors, it seems unlikely that efficient selective mechanisms for its destruction exist in the ISM. (3) Heating in the Solar system – flash-heating is believed to be responsible for the formation of refractory inclusions in meteorites and could have destroyed SiC in the solar nebula; however, this would not account for the lack of SiC in the ISM. So the problem remains unsolved.

Virag et al. (1992) investigated the 'large' meteoritic SiC grains of 1.5–26 μm effective diameter. The first problem, as mentioned above, is the grain size. Conventional theories of circumstellar grain growth cannot produce such large grains. Virag et al. assert that AGB stars (believed to be the source of SiC) with mass-loss rates of typically $< 10^{-5}\,M_\odot\,yr^{-1}$ (Claussen et al. 1987) give an upper size limit for the grain radii of a few hundred ångströms. They also state that optical constraints require that for effective emission at wavelength λ by grains of radius a, $2\pi a$ should be $\ll \lambda$, implying that most of the observed emitting grains are of a size ≤ 0.1 μm (Jura 1990). Constraints on grain size were also discussed by Martin & Rogers (1987), who found a grain size limit of 0.1 μm based on polarization measurements. However, Jura (1994) found that for amorphous carbon grains around the carbon star IRC + 10216, about 1 per cent of the mass must contain particles that are larger than 1 μm in diameter in order to explain the observed circumstellar polarization. He suggested that if the SiC grains have a similar size distribution, then the large SiC grains found in meteorites could originate in the outflows of such stars. Jura, Turner & Balm (1997) have suggested that some AGB/post-AGB stars may have long-lived discs rather than simple outflows. For their example of the Red Rectangle (a post-AGB object), millimetre and submillimetre observations are consistent with orbiting particles of diameter ≥ 0.04 cm at temperatures of about 50 K. This may also explain the meteoritic grain-size problem. However, Griffin (1990) found that his SED modelling required the size of particles around IRC + 10216 to be limited to the range $0.005 \leq \text{radius} \leq 0.05$ μm. Bagnulo, Doyle & Griffin (1995)

used radiative transfer modelling to fit the spectrum of carbon star IRC + 10216. They found that their best fit to the observed *IRAS* LRS spectrum was achieved using only amorphous carbon and no SiC. However, their fit required the grains to have a radius of $\leq 5 \times 10^{-2}$ μm. Such grains obviously cannot account for the meteoritic samples of SiC believed to originate in the outflows of carbon-rich AGB stars. Groenewegen (1997) also performed radiative transfer modelling on the spectrum of IRC + 10216. He found that, rather than using a range of grain sizes, the spectrum was best fitted by assuming a single dominant grain size of about 0.16 μm, and that this seemed to be independent of the exact optical constants used. He also found that grains of 0.1- and 0.35-μm size are needed to explain the polarization observations. He also suggested that very small grains ($\leq$0.08 μm) may not exist around late-type stars. Thus the evidence available is somewhat contradictory. We note that larger grains might be present in carbon star outflows and yet not contribute to the observed infrared feature. However, half the mass of the SiC isolated from the Murchison meteorite is in grains of dimensions $\geq$0.6 μm. Virag et al. invoked planetary nebulae to solve this problem, arguing that the higher mass-loss rate and lower gas expansion rates could lead to environments conducive to the growth of larger grains. However, planetary nebula shells are, in fact, produced near the tip of a star's AGB evolution. This problem is also discussed by Bernatowicz et al. (1996). Virag et al. concluded that, in order to account for the distribution of isotopic compositions, there must be several AGB stars responsible for the production of meteoritic SiC, but that more detailed information on stellar evolution and grain nucleation and growth was needed to make progress.

Alexander (1993) set out to determine how many sources are needed to explain the isotopic compositions of the SiC grains found in meteorites, and whether the isotopic data can be explained by a single AGB star. As an AGB star evolves, its isotopic composition changes. In particular, a ^{13}C-rich star tends towards solar ^{12}C/^{13}C as He-burning produces ^{12}C. However, there is a lack of correlation between the carbon and silicon isotope ratios in meteoritic SiC samples, implying that more than one star is responsible for the isotopes involved. He argued that either most grains come from separate sources, or that there are relatively few sources, with varying isotopic compositions. If the individual sources do not vary isotopically, more than 75 sources would be needed to explain all the isotopic compositions of the grains in this study. Alexander (1993) concluded that between 10 and 100 AGB stars contributed to the SiC in the Solar system. He did not discuss any contributions from novae or supernovae.

Anders & Zinner (1993) have published a review of interstellar diamond, SiC and graphite inclusions in meteorites. Here we focus on the SiC inclusions. They discussed how the various components (i.e., silicon, carbon, nitrogen, noble gases and trace elements) are used to distinguish between the supposed sources, and stated that there are four distinct populations apparent from the carbon and nitrogen isotope data. Three of these can be attributed to the CNO cycle, to He-burning and to explosive H-burning. The isotopic composition of one of these populations led them to conclude that supernovae are the most likely source. However, they pointed out that supernovae would have difficulties growing the micron-sized grains and would not produce enough ^{26}Al. They also discussed the very largest grains (5–20 μm) found in meteorites. These fall into a separate population from the smaller grains, distinct in morphology, crystal structure, and chemical and isotopic trends. These large grains show tight clustering in δ^{29}Si/δ^{28}Si versus ^{12}C/^{13}C space (where the δ notation is a measure of the variation per mil from the standard). One cluster contained only α-SiC and was isotopically normal (terrestrial). It is possible that this group of grains is due to sample contamination. The other two clusters contained only β-SiC grains. The tight clustering of these very large grains may indicate that they come from a small number of source stars. There is no such clustering in the smaller grains. Anders & Zinner argued that the reason for the low abundance of small grains (diameter $\leq$0.4 μm) was not experimental technique, but they did not suggest any other reason. It is possible that there actually is a lack of such small grains.

Pillinger & Russell (1993) investigated many SiC grains, with diameters of up to 23 μm, but typically 1 μm. Most grains gave isotopic data consistent with nucleosynthesis of the elements having occurred via the CNO cycle. These grains are enriched in ^{13}C and depleted in ^{15}N. Other nucleosynthetic signatures found for some grains were: enrichment in both ^{13}C and ^{15}N (attributed to novae), and enrichment in ^{12}C and ^{15}N (believed to be the isotopic signature of supernovae). They concluded that AGB stars were the most likely sources for most of the SiC found in meteorites, with small contributions from novae and supernovae. They did not discuss the grain-size problem.

None of the above papers comments on whether there is a trend in SiC-type with grain size, except that the α-SiC found in the large-grain population is believed to be due to terrestrial contamination, implying that the large grains are all β-SiC (Anders & Zinner 1993). Neither has any comment been made on whether there is any correlation between SiC type and isotopic composition (except for the largest grains). Little progress has been made on the issue of the rarity of SiC grains in the ISM and meteorites. The conclusion we may draw from these papers is that particle size is indeed important. It is possible that the largest grains are formed under special conditions, as supported by Jura et al.'s (1997) findings for the Red Rectangle, and that these grains are formed as β-SiC. For radii significantly larger than 1 μm they would remain undetected in the ISM and in carbon star mid-infrared spectra. However, the majority of circumstellar grains are believed to be small ($\leq$0.1 μm; Jura 1990).

Given that it is geologically unlikely that SiC would form through the processing of solar nebula products in the parent bodies of meteorites, the β-SiC found in meteorites must presumably have a pre-solar origin. It seems probable from the isotopic evidence that some β-SiC is formed by circumstellar grain nucleation around carbon-rich AGB stars. This must have been created as β-SiC, since, from the thermodynamic arguments quoted earlier, α-SiC is unlikely to transform into β-SiC. The evidence from Friedemann et al. (1981), Borghesi et al. (1985) and Pégourié (1988) suggests that the observed 11-μm feature in the spectra of carbon stars matches the laboratory spectrum of α-SiC better then β-SiC. How this is related to the β-SiC found in meteorites (Hoppe et al. 1994) is unknown, although per-

haps the grain-size problem encountered by the meteoriticists is the key.

3 PREVIOUS STUDIES OF THE MID-INFRARED SPECTRA OF CARBON STARS

Hackwell (1972) presented spectra and photometry of 11 M-, S- and C-type stars, only two of which are classed as carbon stars: V Hya and CIT 6. The spectra of both these stars showed a broad feature between 10 and 12 μm, similar to the emission feature calculated by Gilra (1972). This is one of the first published observations of the 11 μm feature, although it was not attributed to SiC by Hackwell (1972). Earlier, however, Hackwell (1971) had concluded on the grounds of condensation sequence studies that SiC was likely to be a major contributor to the circumstellar dust around carbon stars.

Treffers & Cohen (1974) published the mid-infrared spectra of two carbon stars, IRC + 10216 and CIT 6. They found that both stars showed a broad emission band, peaking at about 11.5 μm, which could be fitted very well using model spectra calculated by Gilra for small α-SiC particles having a distribution of shapes. Forrest, Gillett & Stein's (1975) sample of 8–13 μm spectra of cool stars included seven carbon stars, four of which overlap with the present sample. They noted that the SiC feature in the spectra of the carbon stars varied in morphology from star to star. Merrill & Stein (1976) investigated the evolution of the infrared spectra of late-type stars. Their sample consisted of 23 oxygen-rich stars and nine carbon-rich stars (four of which are also included in the present sample). They discussed the 11.5-μm emission feature, attributed to SiC, which had been seen in the spectra of all carbon stars surveyed at that time, and noted that it was unique to carbon stars.

Jones et al. (1978) investigated the infrared source AFGL 3068, which had been suggested by Lebofsky & Rieke (1977) to be the most heavily obscured carbon star known at that time. From its infrared spectrum from 2 to 4 μm and from 8 to 13 μm, Jones et al. (1978) found that (1) there was an absorption feature at 3.1 μm, (2) there was an absence of a silicate feature at 9.7 μm, and (3) there was a spectral break near 10.5 μm. The first two findings confirmed that AFGL 3068 is indeed a heavily dust-enshrouded carbon star. The third discovery was attributed to absorption by SiC grains, the first time that this has been observed. The large SiC grain optical depth indicated by this implies a large mass-loss rate. Jones et al. therefore suggested that if there are many sources like AFGL 3068, they could be major contributors of material to the ISM.

Cohen (1984) presented the mid-infrared spectra of 10 carbon stars. He divided the spectra by appropriate blackbodies to normalize them, in order to see the SiC features more clearly. By doing this he found that there appeared to be two types of features: triangular (narrow and peaked) and rectangular (broader and flatter-topped). The triangular feature could be fitted by a laboratory spectrum of α-SiC from Friedemann et al. (1981). The rectangular feature could not be fitted by any of Friedemann et al.'s laboratory spectra. Cohen suggested that these two distinct features were indicative of different mechanisms of grain formation in different stars, controlled by the mass-loss rates. Alternatively, he suggested that the different feature shapes could arise as a result of different SiC optical depths.

Baron et al. (1987) studied the *IRAS* LRS spectra of 542 carbon stars and came to the following conclusions. (1) The strength of the circumstellar SiC feature is positively correlated with the temperature characterizing the underlying continuum. (2) The shape of the feature varies regularly with its strength and becomes narrower as the strength increases. (3) Weak SiC features are accompanied by an additional bump which peaks at about 8.75 μm; the strongest SiC features are accompanied by a steep rise in the continuum towards 8 μm.

Papoular (1988) studied the *IRAS* LRS spectra of about 3000 carbon stars. Using various smoothing and averaging techniques, he found that the 11-μm features can be divided into three types, which he denoted as SiC(a), SiC(b) and SiC(c). Comparing these separate groups of features to laboratory spectra taken from Borghesi et al. (1985), he found that the different types could be attributed to different laboratory samples. SiC(a) could be fitted by the purest α-SiC with the smallest grains, while SiC(c) was fitted by the least pure α-SiC with the largest grains.

Skinner & Whitmore (1988) discussed the mass-loss rates of carbon stars. They had previously shown that the mass-loss rates of oxygen-rich stars can be determined using the strength of the 9.7-μm silicate dust emission feature. They attempted to employ the same method for carbon stars, using the 11-μm SiC feature, and concluded that the method is reliable. From a sample of 29 carbon stars, they suggested that it is likely that the mass-loss rates increase with the carbon star's age. They also suggested that the amorphous carbon to SiC grain abundance ratio increases with mass-loss rate.

In 1988 Willems published two papers on the *IRAS* LRS spectra of carbon stars (Willems 1988a,b). He found that, for 72 relatively hot carbon stars ($T_{\rm NIR} > 2000$ K), the SiC feature peaked near 11.7 μm in most cases and was accompanied by an unidentified 8.6-μm emission feature, possibly similar to the feature seen by Baron et al. (1987). For 15 cooler carbon stars ($T_{\rm NIR} < 2000$ K) he found that the SiC feature peaked near to 11.3 μm, and concluded that, for these cooler stars, amorphous carbon dust is the main constituent of the circumstellar dust shells.

Goebel et al. (1995) have used SiC and other dust species to create a new classification system for carbon stars. Like Chan & Kwok (1990), they proposed a model explaining the variations in dust types as related to the evolutionary status of the star. They chose to use the α-SiC data of Pégourié (1988) for their model. They proposed that SiC is the first species to condense (because it is very refractory). So, when the star is still relatively hot the contrast of the SiC feature should be very strong. Then, as the star cools and evolves to higher mass-loss rates, newly formed SiC particles form nucleation sites for amorphous hydrogenated carbon (α:C–H). As the star evolves still further and more SiC grains are coated with α:C–H, the SiC feature weakens and a feature appears at about 8.5 μm due to α:C–H. Features in circumstellar spectra due to α:C–H have been discussed before (Puget, Léger & Boulanger 1985; Baron et al. 1987; Skinner & Whitmore 1988). Baron et al. (1987) suggested that,

together with the 8.5-μm feature, there is a feature at 11.7 μm also attributable to α:C–H. If this is true, then both features should appear in spectra when α:C–H is present.

4 TARGET SELECTION

We selected our carbon star targets from a number of source lists. Groenewegen et al. (1992) extended the carbon star infrared classification scheme of Willems & de Jong (1988) by defining five groups of carbon stars. Group I consisted of a small number of J-type carbon stars that exhibit a silicate emission feature. These are not considered further here. Group II sources are those with near-infrared colour temperatures, T_{NIR}, exceeding 2000 K, while Group III sources have T_{NIR} between 1000 and 2000 K. Groups II and III sources have optical counterparts. Group IV sources have T_{NIR} values below 1000 K. Group V sources have the lowest infrared colour temperatures. This sequence was interpreted as one of increasing dust mass-loss rate. 25 of the objects in our sample were amongst the carbon stars having 12-μm *IRAS* fluxes larger than 100 Jy that were classified into these groups by Groenewegen et al. (1992), while Groenewegen (1995) classified another star in our sample, AFGL 5076 (IRAS 02345+5422), as a Group V source. The group classifications of the sources are listed in column 5 of Table 1.

Jura & Kleinmann (1989, 1990) tabulated sources which they classified as very dusty AGB stars. Nine stars in our sample were included in their 1989 listing of sources estimated to be nearer than 1 kpc to the Sun, while eight of our sources were included in their 1990 listing of very dusty carbon-rich sources estimated to be between 1 and 2.5 kpc from the Sun.

Volk, Kwok & Langill (1992) used the *IRAS* LRS data base to identify a group of 32 known or candidate extreme carbon stars. They asserted that these extreme carbon stars have very weak or no SiC features and a relatively low temperature blackbody-like continuum, and so they can be distinguished from 'normal' carbon stars. 10 stars from their sample are included in the present survey. IRAS 02408+5458 was selected from Volk, Kwok & Woodsworth's (1993) list of candidate carbon-rich AGB and post-AGB stars. OH maser emission has been searched for from this source, but not detected (e.g. Blommaert, Van Der Veen & Habing 1993; Wouterloot, Brand & Fiegle 1993). Our 8–13 μm spectrum of it exhibits an 11-μm SiC feature

Table 1. Sources observed.

Source	IRAS names	Other names	Spec. Type*	Group†	Observation Date	Calibrator
IRAS 02152+2822	02152+2822			IV	2/11/93	β Peg
R For	02270–2619	AFGL 337	C3,4e	III	1/11/93	α Lyr
AFGL 341	02293+5748			IV	1&2/11/93	β Peg
AFGL 5076	02345+5422			V	1/11/93	α Tau
IRAS 02408+5458	02408+5458				1/11/93	α Tau
IRC+50096	03229+4721	V838 Per/AFGL 489		III	30/10/93	α Tau
AFGL 5102	03448+4432			IV	1&2/11/93	α Tau
V414 Per	03488+3943	AFGL 527		III	1/11/93	β Peg
R Lep	04573–1452	AFGL 667	C7,4e	III	30/10/93	α Tau
UV Aur	05185+3227	AFGL 735			31/10/93	α Tau
TU Tau	05421+2424	AFGL 812	C5,4		31/10/93	α Tau
UU Aur	06331+3829	AFGL 966	C6,4	II	31/10/93	α Tau
CS 776	07270–1921	AFGL 1131	C8,1e		1/11/93	α CMa
IRC+10216	09452+1330	CW Leo/AFGL 1381	C	IV	17/3/95	β Gem
CIT 6	10131+3049	RW LMi/AFGL 1403	C4,3	III	23/5/91	α Boo
V Hya	10491–2059	AFGL 1439	C7,5e	III	25/5/91	α Boo
Y CVn	12427+4542	AFGL 1576	C7,1e	II	23/5/91	α Boo
AFGL 2155	18240+2326		C	IV	23/5/91	α Boo
IRC+00365	18398–0220	AFGL 2233		III	31/5/91	α Boo
V Aql	19017–0545	AFGL 2314	C5,4	II	1/11/93	α Lyr
AFGL 2333	19075+0921			V	1/11/93	α Lyr
AFGL 2368	19175–0807		C5,4	III	31/5/91	α Lyr
AFGL 2477	19548+3035				31/10/93	α Tau
AFGL 2494	19594+4047			IV	31/11/93	α Lyr
V Cyg	20396+4757	AFGL 2632	C7,4e	III	30/10/93	α Lyr
AFGL 2699	21027+5309	V1899 Cyg	C8,3		30/10/93	β Peg
AFGL 5625	21318+5631			V	2/11/93	α Tau
IRAS 21489+5301	21489+5301			IV	2/11/93	α Lyr
AFGL 3068	23166+1655			V	4/10/90	β Peg
AFGL 3099	23257+1038	IZ Peg	C	IV	1/11/93	β Peg
IRC+40540	23320+4316	LP And/AFGL 3116	C8,3.4	III	30/10 & 2/11/93	β Peg
TX Psc	23438+0312	AFGL 3147	C		1/11/93	β Peg

*From Cohen (1979), Willems (1988a,b), Lorenz-Martin & Lefèvre (1993, 1994) and Blanco et al. (1994).
†From Groenewegen et al. (1992) and Groenewegen (1995).

in absorption (see Section 8), confirming its carbon-rich nature.

5 OBSERVATIONS

Most of the stars in this sample were observed on the nights of 1993 October 30–November 2. The sources CIT 6, V Hya, Y Cvn, AFGL 2233 and AFGL 2368 were observed on the nights of 1991 May 23–31 while AFGL 3068, whose CGS3 spectrum has also been presented by Justtanont et al. (1996), was observed on the night of 1990 October 4. The spectrum of IRC + 10216 was obtained on the night of 1995 March 17 and was kindly made available to us by Dr T. R. Geballe. Table 1 provides some details of the observations. All the observations were made using the 3.8-m United Kingdom Infrared Telescope (UKIRT) with the common-user spectrometer CGS3, a liquid-helium cooled, 10- and 20-μm grating spectrometer built at University College London. CGS3 contains an array of 32 discrete As:Si photoconductive detectors, and three interchangeably, permanently mounted gratings covering the 7.5–13.5 and 16.0–24.5 μm wavebands. Two settings of a grating give a fully sampled 64-point spectrum of the chosen waveband (in the case of IRC + 10216, three settings of the grating gave a 96-point spectrum). We obtained 7.5–13.5 μm spectra with a 5.5-arcsec circular beam and a spectral resolution of 0.17 μm. Further details about CGS3 can be found in Cohen & Davies (1995). Six stars, α Boo, α CMa, α Tau, α Lyr, β Peg and β Gem, were used as flux standards. Table 1 lists the calibrator used for each source. The spectra of sources taken using α Tau as the standard star were flux-calibrated using the absolutely calibrated spectrum of α Tau constructed by Cohen et al. (1992b), whilst several sources were calibrated using a similarly constructed spectrum of β Peg provided by Dr M. Cohen (see Cohen & Davies 1995). A number of sources were calibrated with respect to the A-type stars α Lyr and α CMa, for which Kurucz model-atmosphere calibrations, described by Cohen et al. (1992a), were adopted. Several spectra were calibrated with respect to β Gem and α Boo, which were assumed to emit as blackbodies in the 10-μm region (see Cohen & Davies 1995), with effective temperatures of 4750 and 4450 K respectively. The deep telluric ozone feature at 9.7 μm could not always be completely cancelled; hence in some cases spurious spectral structure could be present in the 9.3–9.8 μm region. The flux-calibrated spectra of all the sources are shown in Fig. 1. The error bars represent 1σ standard errors on the fluxes.

The most prominent characteristic of the flux-calibrated spectra shown in Fig. 1 is the SiC feature, which typically extends from just shortwards of 10 μm to about 12.4 μm. For 26 of the sources the SiC feature is in emission, but for four sources the SiC feature appears to be in absorption. One of these, AFGL 3068, was the only source previously known to exhibit the SiC feature in absorption (Jones et al. 1978), while the other three sources were found to exhibit SiC absorption during the current survey, namely IRAS 02408 + 5458, AFGL 2477 and AFGL 5625. All four of these sources are discussed in more detail in Section 8.

About half of the spectra plotted in Fig. 1 show a marked downturn shortward of 8 μm. This effect was first noticed by Forrest, Gillett & Stein (1975) and, making use of complete spectrophotometry from 0.75 to 13 μm for the carbon star V CrB, Goebel et al. (1981) were able to attribute this downturn to the long-wavelength C_2H_2 wing of a band centred at 7.1 μm due to HCN and C_2H_2. We note that the carbon stars in our sample with optical counterparts tend not to exhibit a downturn. Since the latter sources are likely to correspond to those with higher mass-loss rates, this indicates that the HCN and C_2H_2 molecules apparently responsible for the downturn reside in the outflows.

In the normalized spectra shown in Fig. 2 (see Section 6), in addition to the obvious SiC feature between 10 and 12.5 μm, a weaker emission feature between 8 and 9.5 μm can be discerned in several of the plots, e.g., those of V Aql and Y CVn. This is presumably the same as the feature found in *IRAS* LRS spectra of carbon stars by Baron et al. (1987) and Skinner & Whitmore (1988), and attributed by Papoular (1988) and Goebel et al. (1995) to amorphous hydrogenated carbon. We note that the uncertainty in the true level of the continuum in the 8-μm region, caused by the presence of the HCN/C_2H_2 absorption band shortwards of 8 μm in about half of the sources, may lead to artificial amplification of some of the 8–9.5 μm features during the normalization process.

6 PROPERTIES OF THE SPECTRAL FEATURES

Each of the flux-calibrated spectra was divided by a suitable blackbody, in order to discern more easily the spectral features against the underlying continuum. The blackbodies were chosen by fitting them to the flux-calibrated spectra typically at around 8 and 13 μm. In most cases, the blackbodies used in the normalization process are of approximately the same temperature as those fitted by the χ^2-minimization routine described in the next section. Table 2 gives temperatures of the blackbodies used to normalize the spectra, together with some properties of the 11-μm feature measured on the normalized spectra. The sources are listed in Table 2 in order of increasing 8–13 μm blackbody temperature, which is usually interpreted as a sequence of decreasing mass-loss rate, since stars with very low mass-loss rates ought to show a photospheric continuum, while stars with high mass-loss rates and optically thick dust emission ought to exhibit lower (dust) colour temperatures in the 8–13 μm region. The listed properties of the 11-μm feature are: the feature peak-to-continuum flux ratio, the wavelength of the peak of the feature (λ_{peak}), its full-width at half-maximum (FWHM), full-width at zero-intensity (FWZI), and equivalent width. The peak-to-continuum ratio is the maximum value of the ratio of the intensity in the feature to the underlying continuum intensity. The peak wavelength of the feature is the wavelength at which this peak-to-continuum ratio is measured. Some of the flattened spectra have obvious features at about 8–8.5 μm – possibly due to hydrogenated amorphous carbon (Papoular 1988; Goebel et al. 1995). Stars displaying this feature are AFGL 341, TU Tau, Y CVn, V Aql and AFGL 2699. Fig. 2 shows all the normalized spectra, excluding TX Psc, AFGL 2333 and the spectra with absorption features, which are dealt with later. The five stars mentioned above can be seen to exhibit prominently the 8–8.5 μm features.

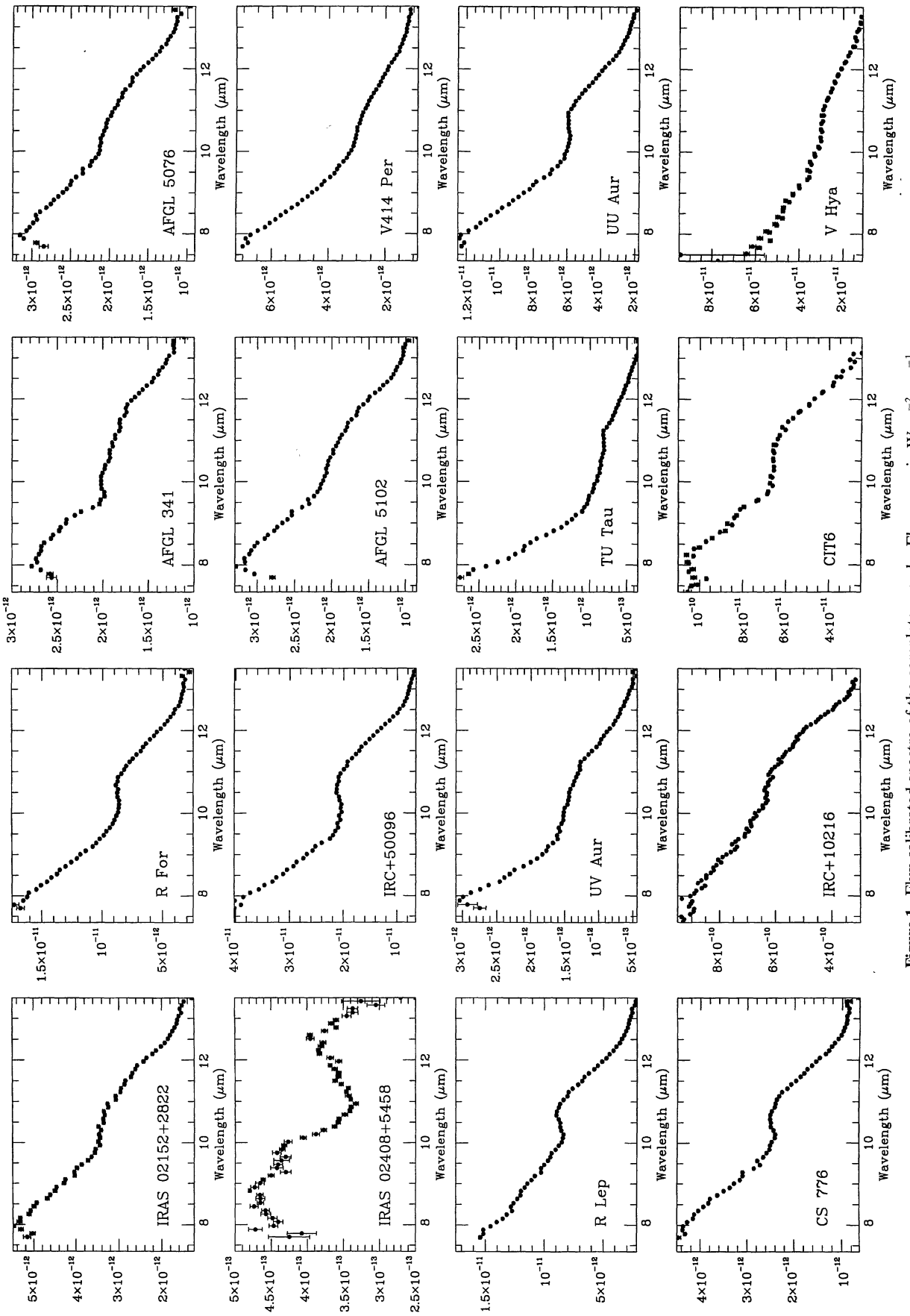

Figure 1. Flux-calibrated spectra of the complete sample. Fluxes are in W m^{-2} μm^{-1}.

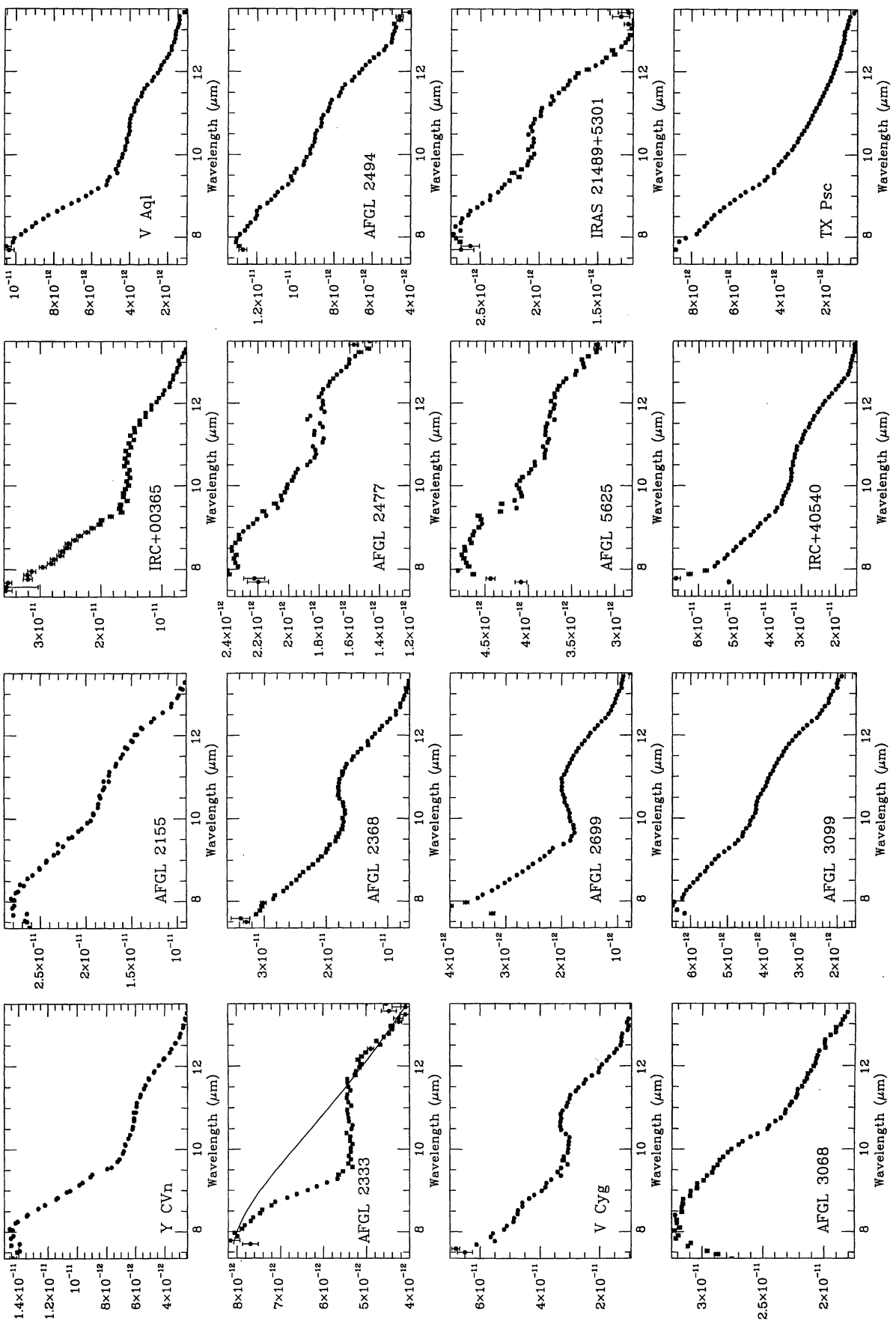

Figure 1 – *continued*

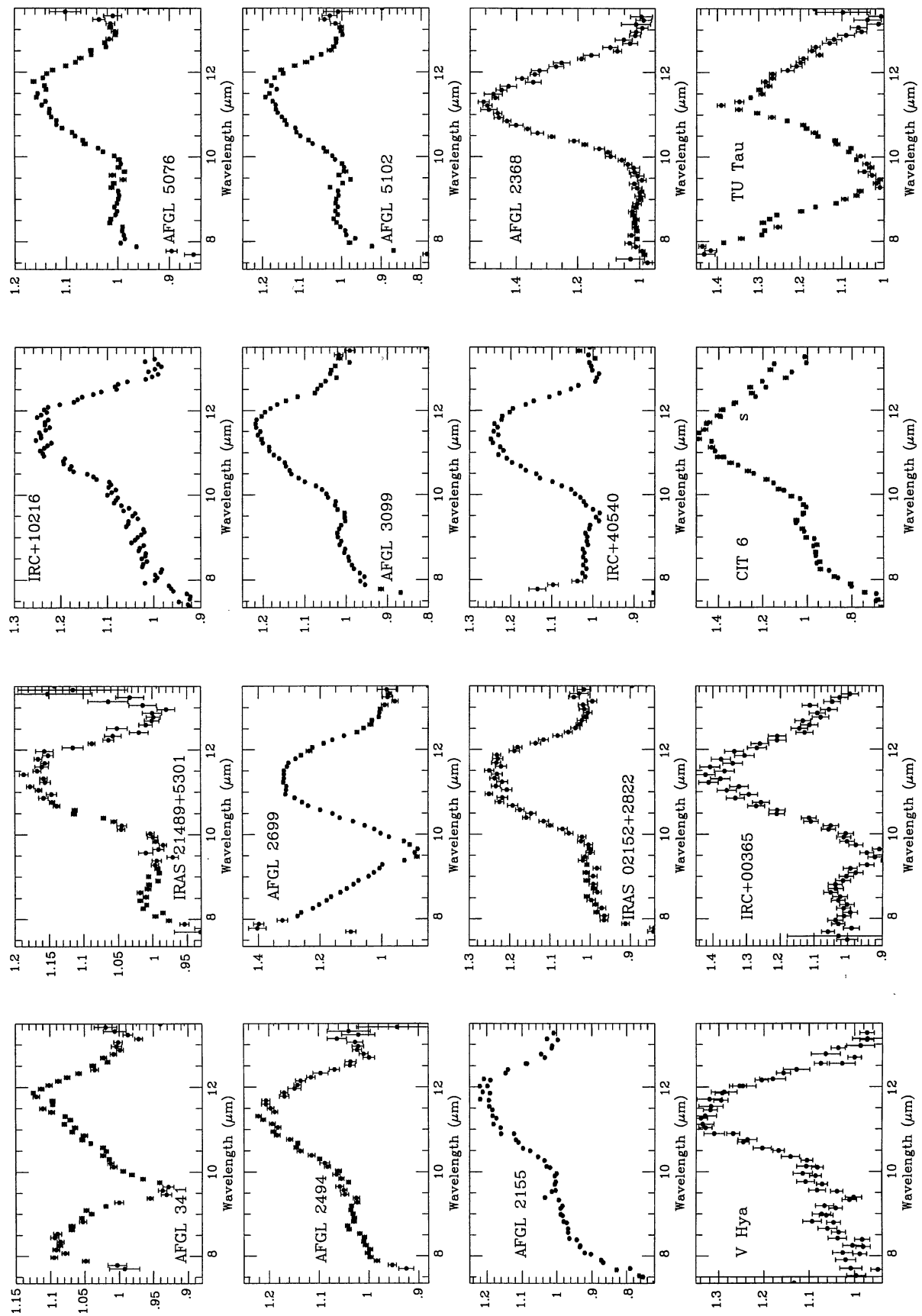

Figure 2. Normalized spectra of the complete sample, excluding TX Psc, AFGL 2333 and the four stars with absorption features.

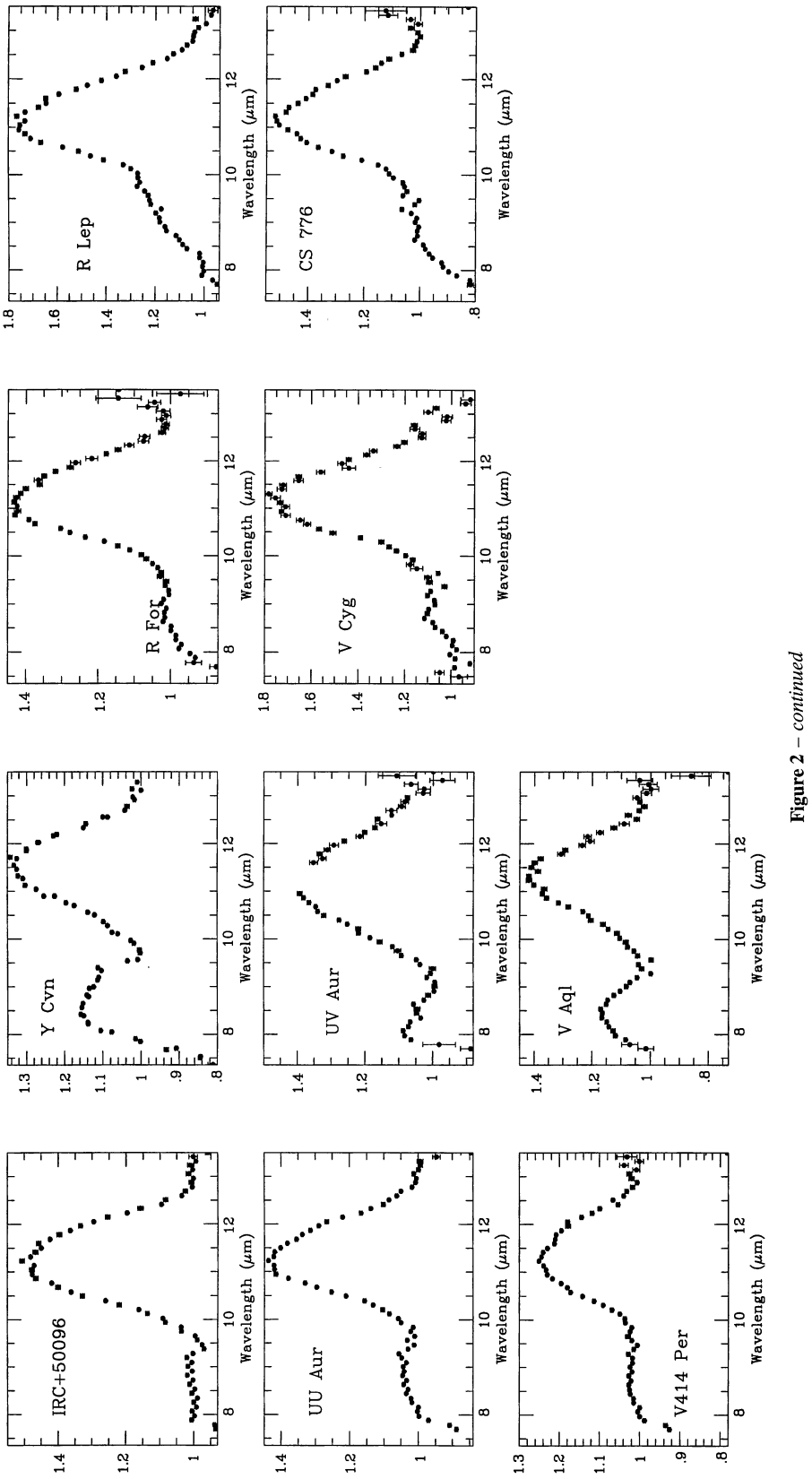

Figure 2 – *continued*

Table 2. Properties of the SiC features measured on the normalized spectra.

Source	Peak/Cont.* Ratio	T_{BB}† (K)	λ_{peak} (μm)	FWHM (μm)	FWZI (μm)	-EW‡ (μm)
IRAS 02408+5458	0.87	320	10.87	1.28	3.23	-0.367
AFGL 5625	0.89	337	10.67	1.96	3.42	-0.055
AFGL 2477	0.85	340	10.56	2.05	3.51	-0.279
AFGL 3068	0.93	377	10.81	1.58	2.54	-0.097
AFGL 341	1.12	410	11.88	1.38	2.76	0.163
IRAS 21489+5301	1.17	455	11.28	1.75	2.69	0.299
IRC+10216	1.24	520	11.45	2.08	4.55	0.557
AFGL 5076	1.14	525	11.45	1.93	2.95	0.275
AFGL 2494	1.15	525	11.29	1.93	3.22	0.296
AFGL 2699	1.32	530	11.27	1.75	3.03	0.553
AFGL 3099	1.21	600	11.64	2.13	3.48	0.404
AFGL 5102	1.18	600	11.50	1.74	3.31	0.329
AFGL 2155	1.19	615	11.72	1.87	2.99	0.386
IRAS 02152+2822	1.23	675	11.33	1.44	3.45	0.459
IRC+40540	1.23	680	11.33	1.93	2.93	0.446
AFGL 2368	1.50	800	11.25	1.85	3.48	0.866
V Hya	1.33	865	11.24	1.74	3.48	0.649
IRC+00365	1.39	975	11.38	1.93	3.24	0.713
CIT6	1.47	1100	11.35	1.84	3.48	0.933
TU Tau	1.39	1100	11.50	2.18	3.58	0.597
IRC+50096	1.47	1200	11.20	1.83	3.06	0.869
Y CVn	1.33	1350	11.55	1.64	2.05	0.573
R For	1.43	1400	11.12	1.74	3.43	0.704
R Lep	1.74	1500	11.13	1.75	4.90	1.609
UU Aur	1.42	1500	11.22	1.65	2.97	0.703
UV Aur	1.46	1500	11.23	1.83	3.85	0.917
V Cyg	1.75	1500	11.29	1.76	4.87	1.508
CS 776	1.58	1600	11.15	1.74	3.32	0.857
V414 Per	1.25	1600	11.24	1.74	3.41	0.423
V Aql	1.40	2250	11.29	1.73	3.49	0.725

*Peak/Cont. = the ratio of the feature intensity to the underlying continuum intensity where the feature strength peaks.
†T_{BB} = temperature of blackbody which gives the best fit to the underlying 8–13 μm continuum.
‡EW = equivalent width.

7 FITTING THE SPECTRA

We have fitted our observed spectra using a χ^2-minimization routine based on one developed for the 10-μm region by Aitken et al. (1979) and Aitken & Roche (1982). The program has been extended by R. J. Sylvester to include the optical constants for six forms of silicon carbide altogether. These are α-SiC from Friedemann et al. (1981); Pég-SiC, a 'synthetic' α-SiC from Pégourié (1988); three different forms of α-SiC (SiC-1200, SiC 600 and SiC-N) from Borghesi et al. (1985); and β-SiC, also from Borghesi et al. (1985). The program is also equipped with the optical constants of silicate from observations of the Orion Trapezium and μCep (see Roche & Aitken 1984).

We attempted to fit all of the spectra taken. AFGL 3068, IRAS 0248+5458, AFGL 2477 and AFGL 5625 all appear to be sources with SiC in absorption and are dealt with in Section 8. All attempted fits involved either a pure blackbody or a blackbody with a λ^{-1} emissivity, together with some form of SiC. For some spectra, the emission fitting routine was unable to provide a satisfactory fit. The spectra cover the 7.5–13.5 μm waveband. There are at least two problems with using the fitting routine over this range. (1) As mentioned above, there may be problems produced by the atmospheric ozone feature at 9.7 μm. Anomalies at this point may produce erroneous solutions from the fitting program. (2) Goebel et al. (1995) have hypothesized that some carbon stars may have amorphous hydrogenated carbon dust in their circumstellar shells, which apparently is the cause of a feature seen in some spectra at about 8.5 μm. At this time the fitting program is not capable of including such a feature in its minimization routine, due to a lack of suitable laboratory data. Spectra which show this feature can mislead the fitting program into asserting that the spectrum in fact has a higher temperature blackbody part, rather than a feature. Thus the fitting program was used several times and in several ways for each spectrum in the sample.

First of all, the routine was used on the flux-calibrated spectra, over the whole range (7.5–13.5 μm) with no alterations. The results are listed in Table 3. The χ^2_R values are the reduced χ^2 values given by dividing the χ^2 value by the number of degrees of freedom. In this case, the minimization routine was unable to find an acceptable fit for TU Tau, V Aql, V Cyg and TX Psc. In order to find fits to these spectra, they were normalized using an appropriate blackbody, the temperature of which is given in the results tables. The χ^2-minimization routine was then applied to these normalized spectra. These results are also found in Table 3, and are denoted by [5]. In the case of TU Tau and UV Aur, the spectra have been edited to avoid the 11–11.5 μm section. This is because there appears to be a narrow 11.25-μm UIR emission band in this region of their spectra (Barlow et al., in preparation).

The second attempt at using the fitting routine was restricted to wavelengths longward of 9.5 μm. The reason for this was to minimize the effects of any features short-

Table 3. Results of the pure emission χ^2-fitting for the 7.5–13.5 μm region of the flux-calibrated spectra.

Source	T_{colour}	BB type	SiC type	T_{BB}(K)	$T_{SiC}(K)$	χ^2_R *
AFGL 341	385	BB*E[1]	SiC-N[2]	884	367	0.490
IRAS 21489+5301	455	BB	SiC-600	457	264	0.684
IRC+10216	520	BB	SiC-600	526	264	1.507
AFGL 5076	525	BB	SiC-600	526	200	0.542
AFGL 2494	525	BB*E	SiC-600	1000	893	0.974
AFGL 2699	530	BB	SiC-N	1563	1180	1.161
AFGL 3099	600	BB	SiC-600	623	223	2.215
AFGL 5102	600	BB	SiC-600	612	234	0.667
AFGL 2155	615	BB	Pég-SiC[3]	569	236	1.370
IRAS 02152+2822	675	BB	SiC-600[2]	671	578	1.074
IRC+40540	680	BB	SiC-600	723	262	0.877
AFGL 2368	800	BB	SiC-600	878	410	1.402
V Hya	865	BB	SiC-600	962	313	1.999
IRC+00365	975	BB	SiC-600	1075	182	1.916
CIT 6	1100	BB	SiC-600	852	279	2.432
TU Tau[4,5]	1100	BB*E	SiC-N	713	181	1.223
IRC+50096	1200	BB	SiC-600	1345	1192	1.561
Y CVn	1350	BB	Pég-SiC	4891	174	1.352
R For	1400	BB	β-SiC[2]	1767	170	2.037
R Lep	1500	BB	β-SiC	2283	267	8.051
UU Aur	1500	BB	β-SiC	2828	173	5.496
UV Aur[4]	1500	BB	β-SiC	1538	208	3.497
V Cyg[5]	1500	BB	SiC-600	291	14	1.984
CS 776	1600	BB	β-SiC	1794	190	3.436
V414 Per	1600	BB	SiC-600	1862	376	0.819
V Aql[5]	2250	BB*E	SiC-N	490	350	1.030
TX Psc	3500	-	——	—	—	—

* χ^2_R is the reduced χ^2 value, i.e., χ^2/n, where n represents the number of degrees of freedom.
[1]BB*E represents a blackbody multiplied by a λ^{-1} emissivity.
[2]'SiC-600', 'SiC-N' and 'β-SiC' are from Borghesi et al. (1985).
[3]'Pég-SiC' is the feature from Pégourié (1988).
[4]TU Tau and UV Aur have been fitted excluding points between 11 and 11.5 μm, to avoid the possible UIR band.
[5]The flux-calibrated spectra of these stars could not be fitted; however, their spectra could be fitted after normalizing them with appropriate blackbodies. The data presented here are for these normalized spectra.

ward of 9.5 μm that might confuse the fitting program (e.g., the 8.5-μm feature). It was not practicable to do the same for the ozone feature at 9.7 μm, as this would have resulted in the loss of part of some of the features. The results are listed in Table 4, and the fits can be seen in Fig. 3 as the dashed lines. This time the fitting program was unable to find solutions for the spectra of R Lep, CS 776, V Aql, V Cyg and TX Psc. Again, for these five sources, the minimization routine was applied to the normalized spectra, and these are the results found in Table 4 for them (denoted by [5]). Although the reduced χ^2 values for the fits listed in Table 4 are not systematically better than those listed in Table 3 for the entire 7.5–13.5 μm region, it was felt that the fits to the SiC features are somewhat more reliable, as fitting over this restricted range of wavelengths avoids any features in the 7.5–9.5 μm region that the program is, as yet, unequipped to deal with.

Cohen (1984) suggested that the shape of some of the features in carbon stars may arise as a result of different SiC optical depths. With this in mind, a third fitting attempt was made, using SiC in both emission and absorption simultaneously, i.e., self-absorbed SiC emission. This self-absorption comprises a warm emitting component and a colder outer component, so that some of the warm 11.3-μm SiC emission is re-absorbed by the cooler dust component. This technique for fitting produced the most interesting results, listed in Table 5. The fits are shown in Fig. 3 as the solid lines. For all but one (V Hya) of the sources with underlying 8–13 μm blackbody temperatures $\leq$1200 K, the χ^2-fitting program was able to find self-absorbed SiC fits. These self-absorption fits are far superior to the fits obtained with SiC only in emission (dashed lines). However, for sources with underlying blackbody temperatures above 1200 K, only one, V414 Per, gave a better fit using SiC self-absorption, the program being unable to find self-absorbed fits to any of the others. The pure emission fits to all the spectra are shown in Fig. 3 (dashed lines) together with, where applicable, the fits using self-absorbed SiC (solid lines). The observed spectra and fits in Fig. 3 have each been divided by a blackbody, whose temperature is listed in Table 2, in order to allow the relative quality of the fits to be more easily discerned. The reduced χ^2 values for the self-absorbed SiC fits are listed in Table 5, and can be seen to be significantly better than the reduced χ^2 values listed in Tables 3 and 4 for SiC purely in emission. The superiority of the self-absorbed SiC fits can also be easily seen from an inspection of Fig. 3.

Groenewegen (1995) fitted α-SiC to the *IRAS* LRS spectra of a number of carbon stars. For the two cases where he

Table 4. Results of the pure emission χ^2-fitting for the 9.5–13.5 μm region of the flux-calibrated spectra.

Source	T_{colour}	BB type	SiC type	T_{BB}(K)	$T_{SiC}(K)$	χ^2_R
AFGL 341	385	BB	SiC-600[1]	411	117	0.749
IRAS 21489+5301	455	BB	SiC-600	450	304	0.880
IRC+10216	520	BB	SiC-N[1]	1061	642	0.881
AFGL 5076	525	BB	SiC-600	533	183	0.714
AFGL 2494	525	BB*E[2]	SiC-600	1550	207	0.670
AFGL 2699	530	BB	SiC-600	507	289	1.937
AFGL 3099	600	BB	SiC-1200[1]	1322	562	1.193
AFGL 5102	600	BB	SiC-600	640	190	0.784
AFGL 2155	615	BB	Pég-SiC[3]	706	129	1.310
IRAS 02152+2822	675	BB	SiC-600	735	323	1.303
IRC+40540	680	BB	SiC-600	759	227	1.164
AFGL 2368	800	BB	SiC-600	1032	311	1.829
V Hya	865	BB	Pég-SiC	1780	240	1.459
IRC+00365	975	BB	SiC-600	882	233	1.739
CIT 6	1100	BB	SiC-600	1331	175	2.273
TU Tau[4]	1100	BB	SiC-600	1768	145	0.652
IRC+50096	1200	BB	SiC-600	1759	584	1.974
Y CVn	1350	BB	SiC-600	4820	138	1.260
R For	1400	BB	β-SiC[1]	3671	150	2.637
R Lep[5]	1500	BB	SiC-600	314	225	1.296
UU Aur	1500	BB	Pég-SiC	5843	656	1.773
UV Aur[4]	1500	BB	SiC-600	3395	544	0.925
V Cyg[5]	1500	BB	SiC-600	288	205	2.357
CS 776[5]	1600	BB	SiC-600	269	253	1.296
V414 Per	1600	BB	SiC-600	643	268	1.043
V Aql[5]	2250	BB*E	SiC-600	358	158	0.848
TX Psc[5]	3500	BB*E	β-SiC	409	68	0.115

[1]'SiC-600', 'SiC-1200', 'SiC-N' and 'β-SiC' are from Borghesi et al. (1985).
[2]BB*E represents a blackbody multiplied by a λ^{-1} emissivity.
[3]'Pég-SiC' is the feature from Pégourié (1988).
[4]TU Tau and UV Aur have been fitted excluding points between 11 and 11.5 μm, to avoid the possible UIR band.
[5]The flux-calibrated spectra of these stars could not be fitted; however, their spectra could be fitted after normalizing them with appropriate blackbodies. The data presented here are for these normalized spectra.

suggested that β-SiC might be present (IRC + 50096 and V Cyg), we find here that α-SiC provides the best fit to our CGS3 spectra.

We note that, apart from the peculiar case of TX Psc (see Section 9), the only source that consistently required to be fitted using β-SiC was R For. The four other sources which apparently required β-SiC when their entire 7.5–13.5 μm spectra were fitted (Table 3) proved to be better fit by α-SiC when the fitting was restricted to the 9.5–13.5 μm region (see Table 4.).

The results for the overall best fits are listed together in Table 6.

8 SOURCES WITH ABSORPTION FEATURES

There are four carbon star spectra in our sample which exhibit net absorption features. AFGL 3068 and IRAS 02408 + 5458 both show evidence of a broad absorption band in the 10–12.5 μm region. AFGL 3068 was originally investigated by Jones et al. (1978), who concluded that this feature was due to SiC in absorption. IRAS 02408 + 5458 has a very similar, but much stronger, feature than AFGL 3068, as may be seen from a comparison of Figs 4(a) and (d).

AFGL 2477 and 5625 also show evidence of absorption features, only this time they appear to have a double absorption peak (see Figs 4b and c). The longer wavelength feature is very similar to that seen in the spectra of AFGL 3068 and IRAS 02408 + 5458. The shorter wavelength feature is centred at about 9.7 μm. Incomplete cancellation of telluric ozone absorption may contribute to this peak, but the absorption appears to extend, on both sides, well beyond the 9.3–9.9 μm region affected by ozone. Both these stars had their spectra calibrated using several different standard stars which were observed on the same night, and the short-wavelength extended absorption was found to persist. For this reason we believe that this feature is real. One possibility is that it is due to interstellar silicate absorption.

We applied the χ^2-minimization routine to both the flux-calibrated and to the normalized spectra in a variety of ways. In addition to fitting the spectra with (1) a single form of SiC, fitting was also attempted on the normalized spectra using (2) a combination of one SiC variant and an interstellar silicate, (3) a combination of two different types of SiC and an interstellar silicate. Then, following the success of fitting the emission features using self-absorbed SiC, the absorption features were also fitted (4) using self-absorbed silicon carbide and (5) self-absorbed SiC with an interstellar silicate. The results of fits (1)–(3) to the normalized spectra, together with the SiC self-absorption fits (4) and (5) to the

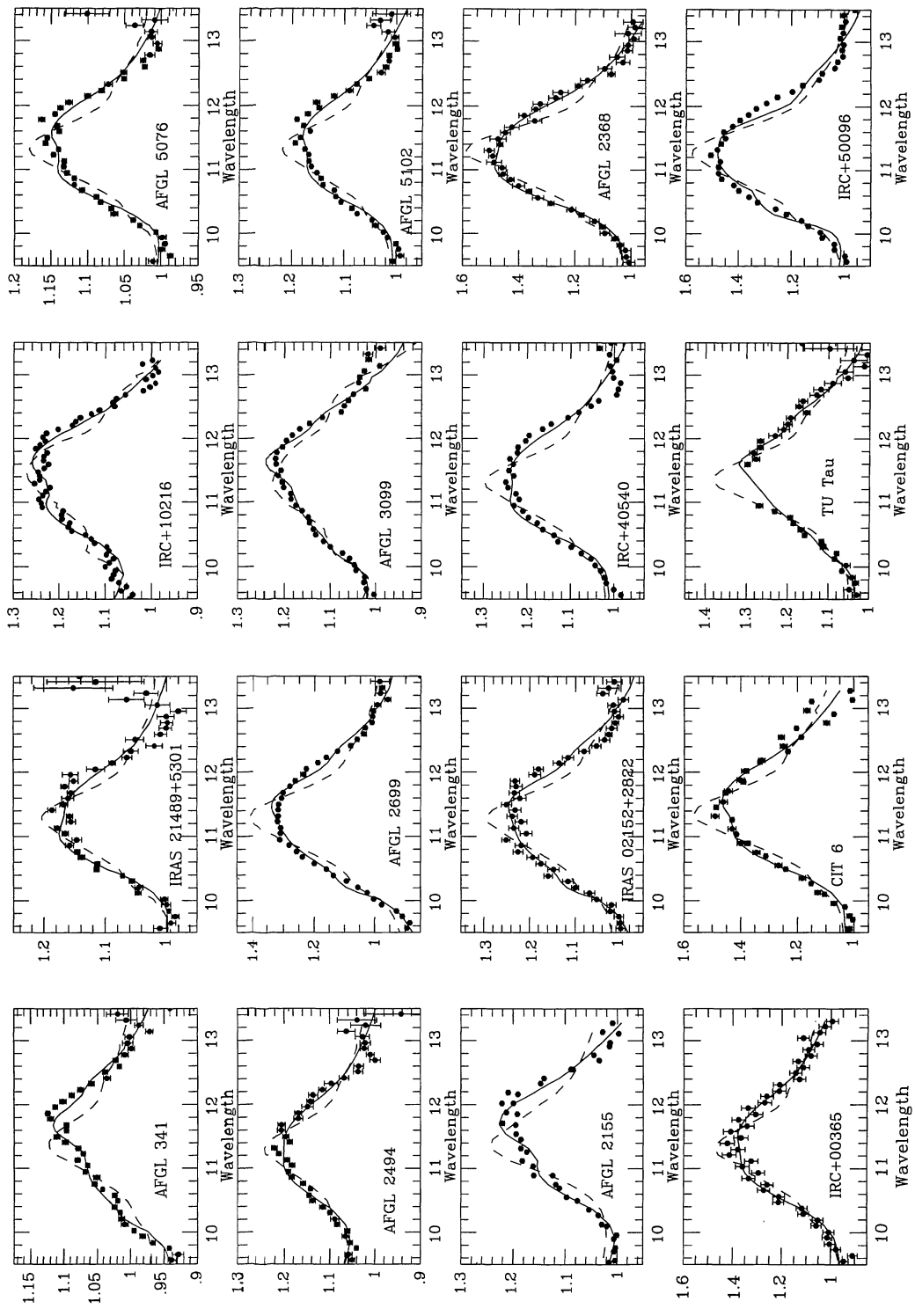

Figure 3. SiC self-absorption fits (solid lines) and 'pure emission' fits (dashed lines) to the flux-calibrated spectra normalized to show details.

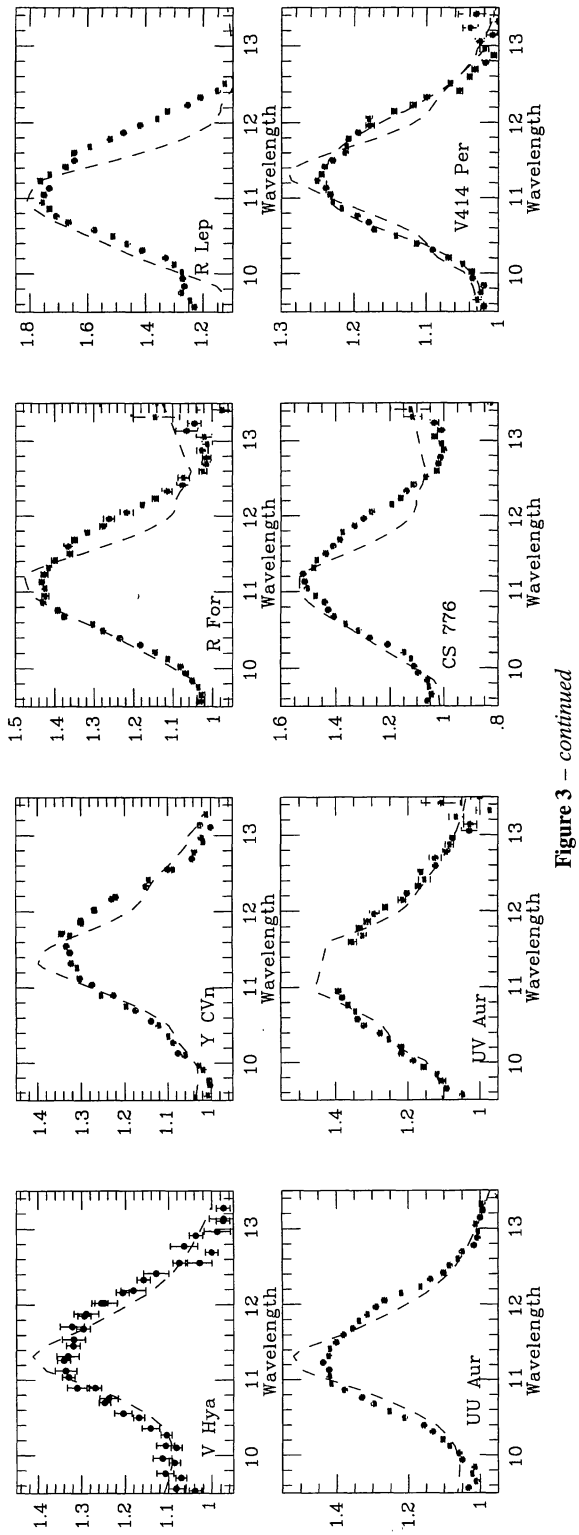

Figure 3 – *continued*

flux-calibrated spectra, are listed in Table 7. The fits obtained using self-absorbed SiC proved to be very good, with plausible optical depths. Fitting using both SiC and interstellar silicate only yields fits for AFGL 2477 and 5625. We have already discussed the possibility that the spectra of these two stars are affected by interstellar silicate absorption. Self-absorption fits using SiC only are shown in Fig. 5; fits using self-absorbed SiC and interstellar silicate absorption are shown in Fig. 6.

For cases (1)–(3), it was found to be necessary first to normalize the flux-calibrated spectra, by dividing by an appropriate blackbody, before a fit could be obtained. When carrying out pure absorption fits, β-SiC was always found to be needed (Table 7a). However, although β-SiC fitted the wavelength of the peak absorption well, the model absorption profile was always found to be too narrow compared to the observed widths, with excess absorption still remaining on both sides of peak. A combination of absorption by β-SiC plus interstellar silicate absorption (with a Trapezium silicate profile in the case of AFGL 3068, and a μ Cep silicate profile for the rest) gave a much better fit in all cases (Table 7b). However, significant excess absorption still remained unfitted in the red wings of the observed profiles. The inclusion of absorption by α-SiC (which peaks at a longer wavelength than that from β-SiC) allowed this excess absorption to be fitted. Table 7(c) lists the χ^2 best-fitting parameters for each object for this case of absorption by interstellar silicate and two forms of SiC (β and α).

The values listed in Table 7(c) for $\tau_{9.7}$, the optical depth at 9.7 μm due to interstellar silicate absorption, show a rather narrow range of 0.15–0.21. For an adopted value of $A_V/\tau_{9.7}=18.5$ (Roche & Aitken 1984), these 9.7-μm optical depths correspond to values of A_V between 2.7 and 3.9 mag, which appears plausible in the light of previous estimates for the interstellar extinction to these stars (e.g. Groenewegen 1995). However, a possible drawback to these three-component absorption fits (apart from the need to normalize the spectra first) lies in the fact that in each case the interstellar silicate 9.7-μm optical depth comes out as significantly larger than the optical depths of either of the SiC absorption components. Given that we earlier (Section 7) found that the carbon stars with 8–13 μm colour temperatures of less than 1200 K all required some SiC self-absorption to provide a good fit to their observed net emission profiles, it seems plausible that any fit to a SiC profile that is in net absorption should also invoke SiC self-absorption, i.e., absorption by cooler SiC particles, situated further out in the outflow, of an SiC emission feature produced by warmer SiC particles situated deeper in the flow. We therefore also experimented with fitting the flux-calibrated spectra by a blackbody continuum plus a single type of self-absorbed SiC. The results are listed in Table 7(d) and are plotted (after normalization) in Fig. 5. In each case, self-absorbed α-SiC was found to yield the best fit, managing to fit the wavelengths of peak absorption and the observed widths of the overall absorption profiles. The reduced χ^2 values for self-absorbed α-SiC (Table 7d) are very similar to the reduced χ^2 values obtained for pure absorption of a blackbody by two forms of SiC plus interstellar silicate absorption, (Table 7c). Given that SiC self-absorption appears to be the more physically plausible scenario, we therefore prefer the fits obtained with the former assump-

Table 5. Results of the χ^2-fitting for the 9.5–13.5 μm region of the flux-calibrated spectra using self-absorbed SiC.

Source	T_{colour}	BB type	SiC type	T_{BB}(K)	T_{SiC}(K)	τ_{SiC}	χ^2_R
AFGL 341	385	BB	SiC-600[1]	420	265	0.189	0.227
IRAS 21489+5301	455	BB*E[2]	Pég-SiC[3]	837	546	0.398	0.568
IRC+10216	520	BB	Pég-SiC	828	331	0.537	0.345
AFGL 5076	525	BB*E	Pég-SiC	1337	439	0.421	0.714
AFGL 2494	525	BB*E	Pég-SiC	1899	474	0.385	0.401
AFGL 2699	530	BB*E	SiC-600	1381	333	0.197	0.460
AFGL 3099	600	BB	SiC-600	918	288	0.216	1.124
AFGL 5102	600	BB	Pég-SiC	685	468	0.422	0.361
AFGL 2155	615	BB	Pég-SiC	944	287	0.541	1.310
IRAS 02152+2822	675	BB	SiC-600	795	439	0.172	0.606
IRC+40540	680	BB	Pég-SiC	685	468	0.422	0.361
AFGL 2368	800	BB	Pég-SiC	1421	1160	0.519	0.347
V Hya	865	–	——-	—	—	—–	—–
IRC+00365	975	BB	Pég-SiC	1121	625	0.512	1.739
CIT 6	1100	BB	Pég-SiC	3116	480	0.560	0.855
TU Tau[4]	1100	BB	SiC-600	2120	296	0.174	0.369
IRC+50096	1200	BB	α-SiC[5]	3884	1493	0.649	1.157
Y Cvn	1350	–	——-	—	—	—–	—–
R For	1400	–	——-	—	—	—–	—–
R Lep	1500	–	——-	—	—	—–	—–
UU Aur	1500	–	——-	—	—	—–	—–
UV Aur	1500	–	——-	—	—	—–	—–
V Cyg	1500	–	——-	—	—	—–	—–
CS 776	1600	–	——-	—	—	—–	—–
V414 Per	1600	BB	Pég-SiC	3360	1406	0.420	0.526
V Aql	2250	–	——-	—	—	—–	—–
TX Psc[6]	3500	BB	SiC-1200	326	222	0.012	1.455

[1]'SiCCC-600' is from Borghesi et al. (1985).
[2]BB*E represents a blackbody multiplied by a λ^{-1} emissivity.
[3]'Pég-SiC' is the feature from Pégourié (1988).
[4]TU Tau and UV Aur have been fitted excluding points between 11 and 11.5 μm, to avoid the possible UIR band.
[5]'α-SiC' is from Friedemann et al. (1981).
[6]The flux-calibrated spectrum of TX Psc could not be fitted; however, the spectrum could be fitted after normalization with 3500-K blackbodies. The data presented here are for the normalized spectrum.

Table 6. Summary of the best χ^2-fits.

Source	T_{BB} (K)	Peak/Cont. ratio	SiC type(1)	SiC type(2)	SiC type(3)	τ_{SiC}
AFGL 341	385	1.15	SiC-N	SiC-600	SiC-600	0.189
IRAS 21489+5301	455	1.17	SiC-600	SiC-600	Pég-SiC	0.398
AFGL 2699	475	1.41	SiC-N	SiC-600	SiC-600	0.197
IRC+10216	520	1.24	SiC-600	SiC-N	Pég-SiC	0.537
AFGL 5076	525	1.14	SiC-600	SiC-600	Pég-SiC	0.421
AFGL 2494	525	1.15	SiC-600	SiC-600	Pég-SiC	0.385
AFGL 3099	600	1.21	SiC-600	SiC-1200	SiC-600	0.216
AFGL 5102	600	1.18	SiC-600	SiC-600	Pég-SiC	0.422
AFGL 2155	615	1.19	Pég-SiC	Pég-SiC	Pég-SiC	0.541
IRAS 02152+2822	675	1.23	SiC-600	SiC-600	SiC-600	0.172
IRC+40540	680	1.23	SiC-600	SiC-600	Pég-SiC	0.422
AFGL 2368	800	1.50	SiC-600	SiC-600	Pég-SiC	0.519
V Hya	865	1.33	SiC-600	Pég-SiC	—–	—–
IRC+00365	975	1.39	SiC-600	SiC-600	Pég-SiC	0.512
CIT 6	1100	1.47	SiC-600	SiC-600	Pég-SiC	0.560
TU Tau	1100	1.29	—–	SiC-600	SiC-600	0.174
IRC+50096	1200	1.47	SiC-600	SiC-600	α-SiC	0.649
Y Cvn	1350	1.33	Pég-SiC	SiC-600	—–	—–
R For	1400	1.43	β-SiC	β-SiC	—–	—–
R Lep	1500	1.74	β-SiC	—–	—–	—–
UU Aur	1500	1.42	β-SiC	Pég-SiC	—–	—–
UV Aur	1500	1.46	β-SiC	SiC-600	—–	—–
V Cyg	1500	1.75	SiC-600*	SiC-600*	—–	—–
CS 776	1600	1.58	β-SiC	SiC-600*	—–	—–
V414 Per	1600	1.25	SiC-600	SiC-600	Pég-SiC	0.420
V Aql	2250	1.40	SiC-N*	SiC-600*	—–	—–
TX Psc	3500	—-	—–	—–	—–	—–

SiC-Type (1) is taken from the χ^2-fitting data of the flux-calibrated spectra over 7.5–13.5 μm.
SiC-Type (2) is taken from the χ^2-fitting data of the flux-calibrated spectra over 9.5–13.5 μm.
SiC-Type (3) is taken from the self-absorption χ^2-fitting data. τ_{SiC} is the optical depth of the SiC taken from the self-absorption χ^2-fitting data.
*These data came from fits to normalized spectra.

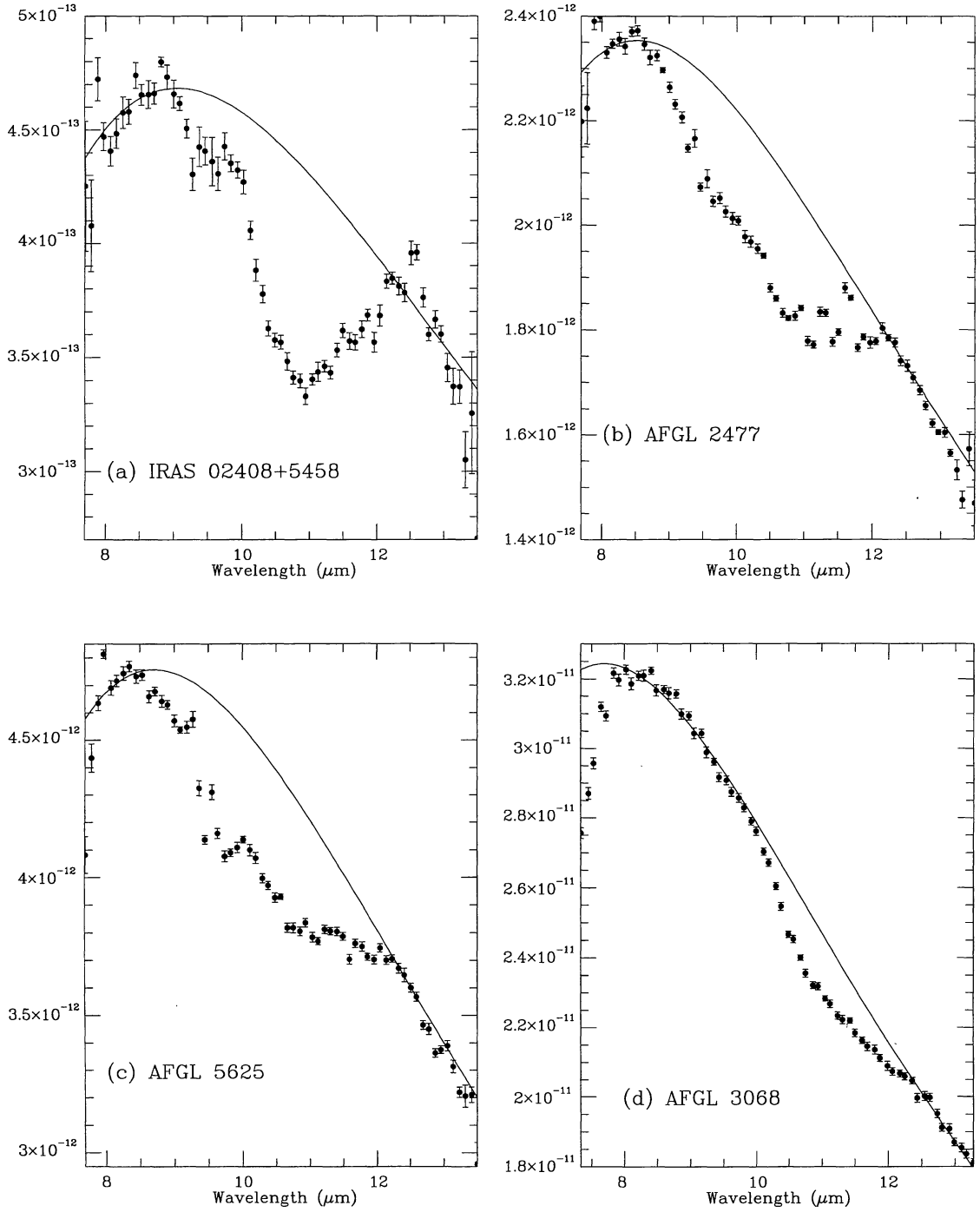

Figure 4. Flux-calibrated spectra of four sources showing absorption features, together with the blackbodies used for normalization.

tion. We have also obtained fits using self-absorbed SiC with interstellar silicate. In this case only AFGL 2477 and 5625 can be fitted. Slightly better χ^2-fits were obtained than for SiC self-absorption alone, and the fits are shown in Fig. 6. The interstellar silicate absorption was required to have a μ Cep profile, rather than a (broader) Trapezium profile.

The perplexing source AFGL 2477 is of some additional interest. Groenewegen et al. (1996a) found the optical counterpart to be an oxygen-rich M6S star, but that the dominant mid-infrared spectrum closely resembled that of a heavily obscured carbon star, with the observed millimetre-wave CO/HCN line flux ratio and the lack of OH maser emission as supporting evidence for the presence of a carbon star. They suggested that the M6S star, visible at optical wavelengths, was either (1) a first-ascent red giant star with an A_V (circumstellar and interstellar) of 2.1–2.4 mag, located within 5 arcsec of an optically obscured AGB carbon star companion, or (2) a distant oxygen-rich AGB star which happens to be projected within 5 arcsec of a much closer optically obscured carbon star. The presence of an

Table 7. Results of the χ^2-fitting for the normalized spectra exhibiting absorption features.

(a) χ^2-fits to absorption features using a single form of SiC in pure absorption

Source	BB type	SiC type	T_{BB}(K)	τ_{SiC}[2]	χ^2_R
IRAS 02408+5458	BB*E[1]	β-SiC	378	0.067	2.433
AFGL 5625	BB*E	β-SiC	357	0.060	3.333
AFGL 2477	BB*E	β-SiC	359	0.067	3.132
AFGL 3068	BB	β-SiC	367	0.052	1.096

(b) χ^2-fits to absorption features using a single form of SiC and an interstellar silicate, all in pure absorption.

Source	BB type	SiC type	T_{BB}(K)	τ_{SiC}	$\tau_{9.7}$[5]	χ^2_R
IRAS 02408+5458	BB	β-SiC	383	0.097	0.128	1.179
AFGL 5625	BB*E	β-SiC	366	0.033	0.195	0.356
AFGL 2477	BB*E	β-SiC	367	0.041	0.190	0.321
AFGL 3068	BB*E	β-SiC	373	0.097	0.123	0.429

(c) χ^2-fits to absorption features using two forms of SiC and an interstellar silicate, all in pure absorption.

Source	BB type	SiC type1	SiC type2	T_{BB}(K)	τ_{SiC1}[3]	τ_{SiC2}[4]	$\tau_{9.7}$	χ^2_R
IRAS 02408+5458	BB*E	β-SiC	Pég-SiC	371	0.074	0.064	0.153	0.905
AFGL 5625	BB*E	β-SiC	Pég-SiC	361	0.021	0.035	0.208	0.274
AFGL 2477	BB*E	β-SiC	Pég-SiC	362	0.028	0.035	0.203	0.236
AFGL 3068	BB*E	β-SiC	SiC-1200	346	0.015	0.042	0.191	0.093

(d) χ^2-fits to absorption features using self-absorbed SiC

Source	BB type	SiC type	T_{BB}(K)	T_{SiC}(K)	τ_{SiC}	χ^2_R
IRAS 02408+5458	BB	SiC-600	345	86	0.128	1.073
AFGL 5625	BB	SiC-1200	397	193	0.126	0.295
AFGL 2477	BB*E	SiC-600	514	74	0.041	0.360
AFGL 3068	BB	α-SiC	387	66	0.099	0.091

(e) χ^2-fits to absorption features using self absorbed SiC and an interstellar silicate absorption feature.

Source	BB type	SiC type	T_{BB}(K)	T_{SiC}(K)	τ_{SiC}	$\tau_{9.7}$	χ^2_R
IRAS 02408+5458	–	——-	—	–	—	—	—
AFGL 5625	BB	Pég-SiC	346	139	0.192	0.084	0.275
AFGL 2477	BB	Pég-SiC	358	127	0.218	0.072	0.256
AFGL 3068	–	——-	—	–	—	—	—

[1]BB*E represents a blackbody multiplied by a λ^{-1} emissivity.
[2]τ_{SiC} is the optical depth of the SiC.
[3]τ_{SiC1} is the optical depth of β-SiC.
[4]τ_{SiC2} is the optical depth of SiC type 2.
[5]$\tau_{9.7}$ is the optical depth of the interstellar silicate.

SiC absorption feature in our 8–13 μm spectrum of AFGL 2477 (Figs 4b, 5b and 6a) supports the attribution of the mid-infrared emission of AFGL 2477 to a carbon star. If we adopt an interstellar ratio of $A_V/\tau_{9.7}=18$ (Roche & Aitken 1984), the silicate $\tau_{9.7}$ of 0.072 that we observe implies an interstellar A_V of 1.3 mag toward AFGL 2477.

9 TX PSC

TX Psc is the only carbon star in the sample for which the χ^2-fitting routine consistently had problems finding fits to the spectrum. For this reason the spectrum of TX Psc needed further investigation. Its flux-calibrated spectrum is shown in Fig. 7(a). The best-fitting 8–13 μm blackbody has a temperature of 3500 K. Dividing by this blackbody yields a normalized spectrum which does not show an obvious 11-μm feature (Fig. 7b). It does, however, exhibit a prominent feature at 8.8 μm. This could be the usual feature found in this region, attributed to α:C–H. The 3500-K blackbody does not fit perfectly, so that the 'normalized' spectrum in Fig. 7(b) does not have a flat underlying continuum. The resulting spectrum has peaks at 8.8 and 11.3 μm (Fig. 7b). It would appear that the spectrum of TX Psc may have contributions from three sources: (1) a hot 3500-K photospheric continuum; (2) a feature at 8.8 μm, possibly due to α:C–H; and (3) a weak feature at 11.3 μm , possibly due to SiC. We were able to obtain a fit to the flux-calibrated 7.5–13.5 μm spectrum using self-absorbed α-SiC (although the 8.8-μm feature could, of course, not be fitted). This fit is shown in Fig. 7(c), where both the spectrum and the fit have been divided by a 3500-K blackbody. The best-fitting parameters are listed in Table 5. TX Psc can be seen to be unusual, since it has by far the highest 8–13 μm colour temperature and yet can be fitted by self-absorbed SiC. How this star fits into the evolutionary scheme of carbon stars is unknown. In any case, it is clear that the mid-infrared spectrum of TX Psc is markedly different from those of other carbon stars in our sample. We note that the only fit that could be obtained to the normalized 9.5–13.5 μm spectrum was with β-SiC; this is shown in Fig. 7(d).

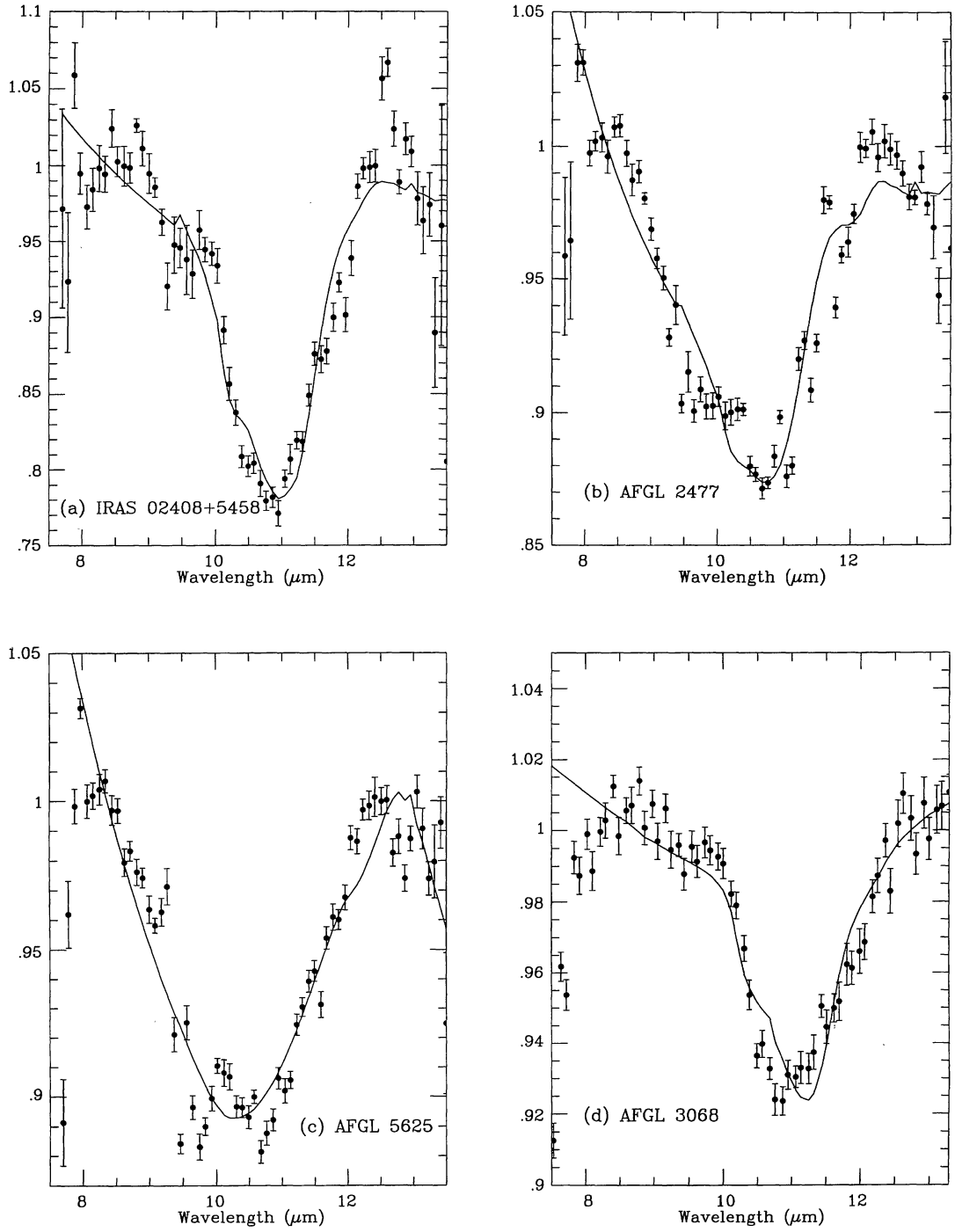

Figure 5. Flux-calibrated spectra of sources showing absorption features with best χ^2-fits using self-absorbed SiC (normalized for display).

10 AFGL 2333

AFGL 2333 was originally included in our sample as it has been classified as a carbon star based on its *IRAS* LRS spectrum and HCN emission (Groenewegen et al. 1992; Loup et al. 1993; Volk et al. 1992, 1993). However, on the basis of its OH maser emission (see Le Squeren et al. 1992 and David et al. 1993), we believe that it is an OH/IR star. The flux-calibrated spectrum of AFGL 2333 is included with those of the rest of the sample in Fig. 1, and shows that the spectrum in fact exhibits an absorption feature centred at about 9.6 μm rather than an emission feature at about 11.5 μm. AFGL 2333 can therefore be interpreted as an oxygen-rich OH/IR star that exhibits silicate self-absorption. The spectrum of AFGL 2333 can be fitted very well using self-absorbed silicate. The minimization routine gave a reduced χ^2 value of 0.265 using a Trapezium silicate profile, with an optical depth of 1.51. The fit is shown in Fig. 8.

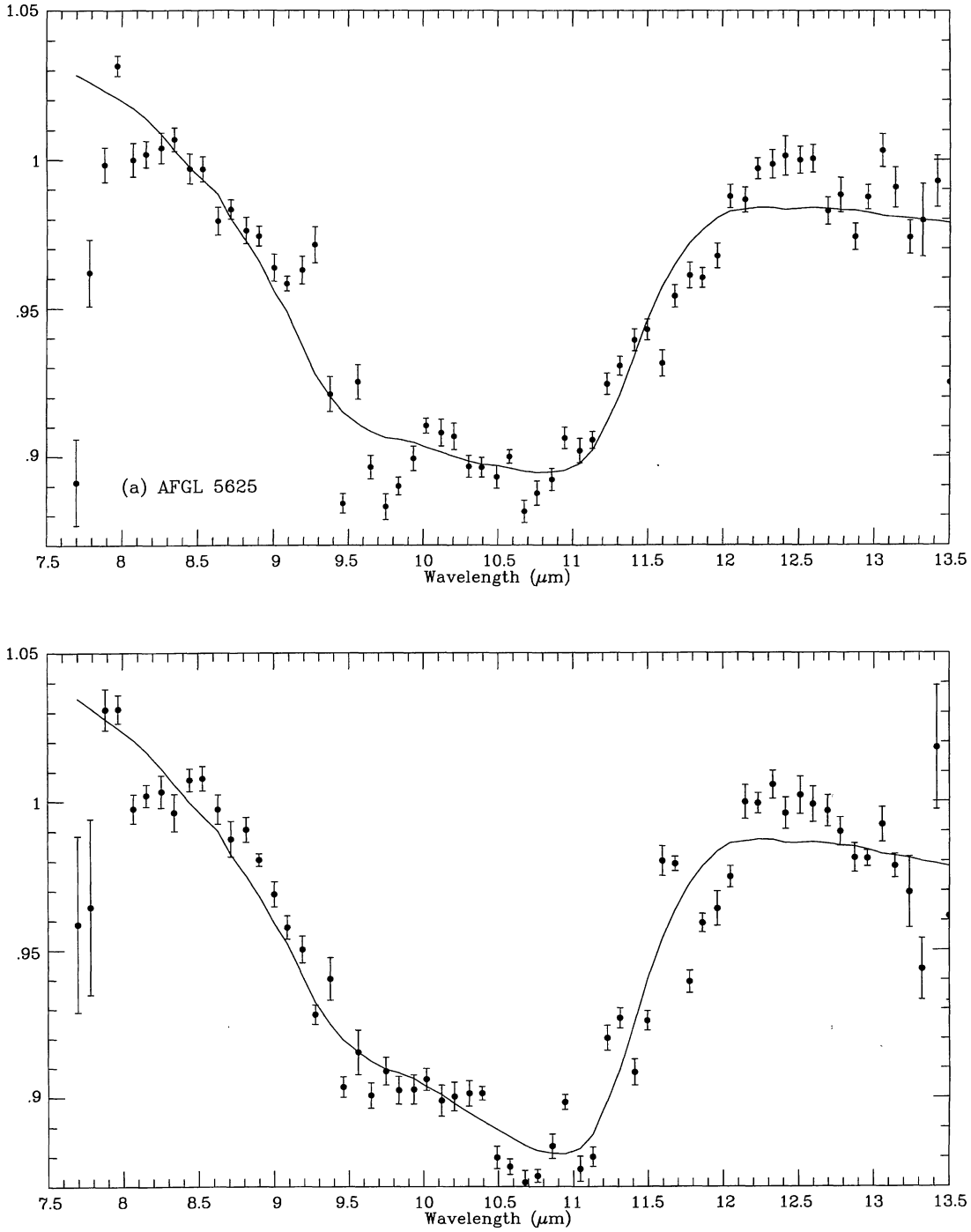

Figure 6. Flux-calibrated spectra of sources showing absorption features with best χ^2-fits using self-absorbed SiC and interstellar silicate feature (normalized for display).

11 DISCUSSION

Fig. 9 uses some of the SiC feature parameters listed in Table 2 with a view to finding trends in the SiC features. In each plot (a–c), the solid line represents a linear regression fit to the plotted data.

We found no correlation between the FWHM of the SiC profile and the 8–13 μm colour temperature (the formal linear correlation coefficient is −0.241) or between the full width at zero intensity (FWZI) of the SiC profile and the colour temperature (the linear correlation coefficient is 0.312). An attempt was made to find correlations between the stellar mass-loss rates and the properties of the 8–13 μm spectra. The mass-loss data were taken from Jura (1986), Jura & Kleinmann (1989), Loup et al. (1993) and Volk et al. (1993). Published mass-loss rates were found for 25 of our sources. The only combination of data that yielded any correlation was that of the mass-loss rates of Loup et al. (1993) versus the 8–13 μm colour temperature. The plot excludes the mass-loss rates for the four stars whose spectra

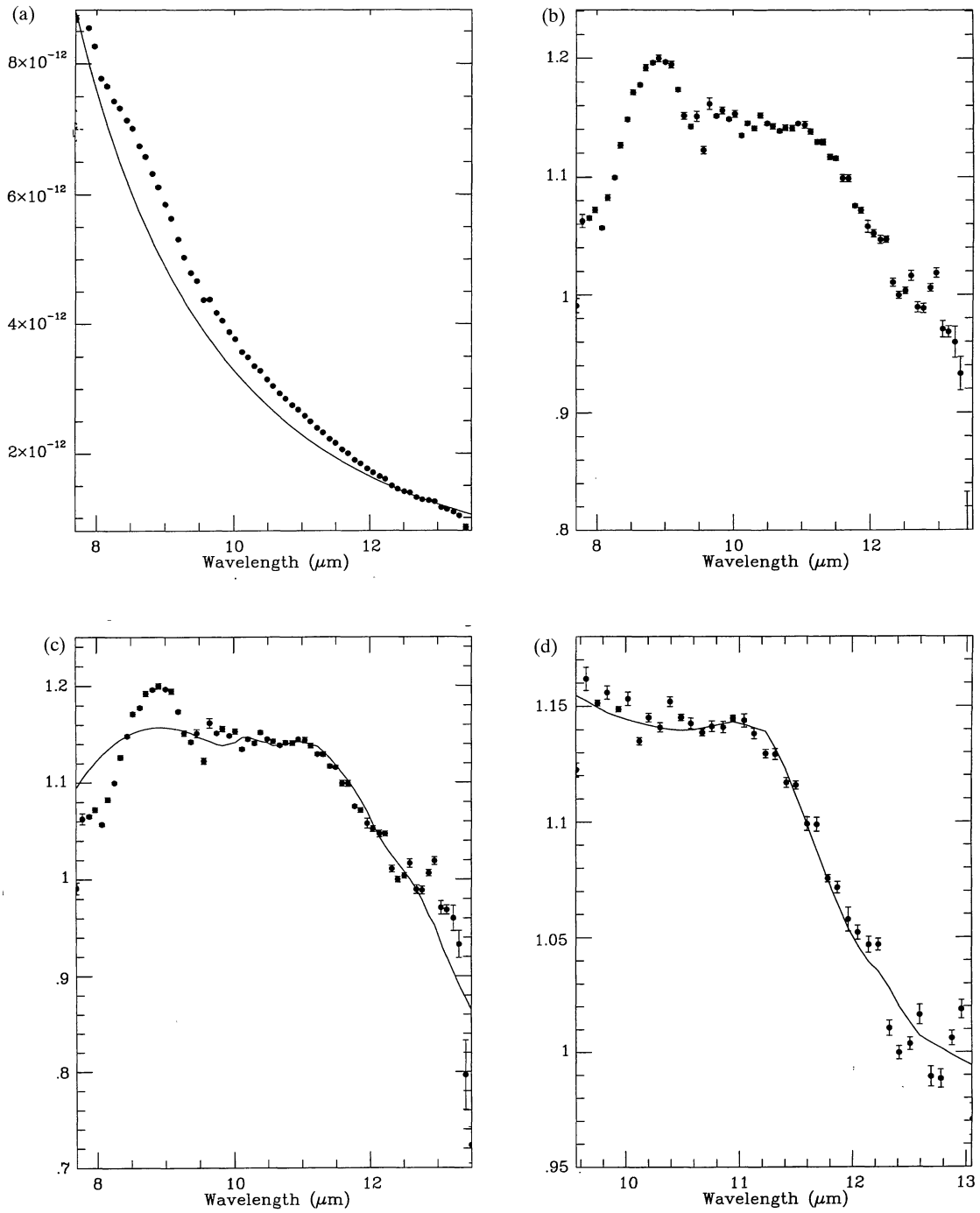

Figure 7. TX Psc. (a) Flux-calibrated spectrum of TX Psc with best-fitting 3500-K blackbody. (b) Spectrum of TX Psc after division by a 3500-K blackbody. (c) Spectrum of TX Psc after normalization by a 3500-K blackbody together with the best χ^2 fit (for the 7.5 to 13.5 μm region) using self-absorbed SiC (the fit utilizes α-SiC). (d) Spectrum of TX Psc after normalization by a 3500-K blackbody, together with the best χ^2 fit for the 9.5 to 13.0 μm region (the fit utilizes β-SiC purely in emission).

exhibit absorption features, as well as TX Psc. The resulting correlation can be seen in Fig. 9(a). The linear correlation coefficient is −0.605. It can be seen that as the mass-loss rate increases, the underlying continuum colour temperature decreases. This is as expected for dust shells that become increasingly optically thick as the mass-loss rate increases. Fig. 9(b) shows the SiC peak wavelength (i.e., the wavelength at which the ratio of the flux of the feature to the flux of the underlying continuum is highest) versus the colour temperature of the underlying 8–13 μm continuum. There is no correlation (the formal linear correlation coefficient for the best straight-line fit through the data is 0.11). This lack of correlation between the peak wavelength of the feature and the 8–13 μm colour temperature disagrees with the findings of Willems (1988a,b). Fig. 9(c) shows a plot of the SiC peak-to-continuum ratio versus the underlying 8–13

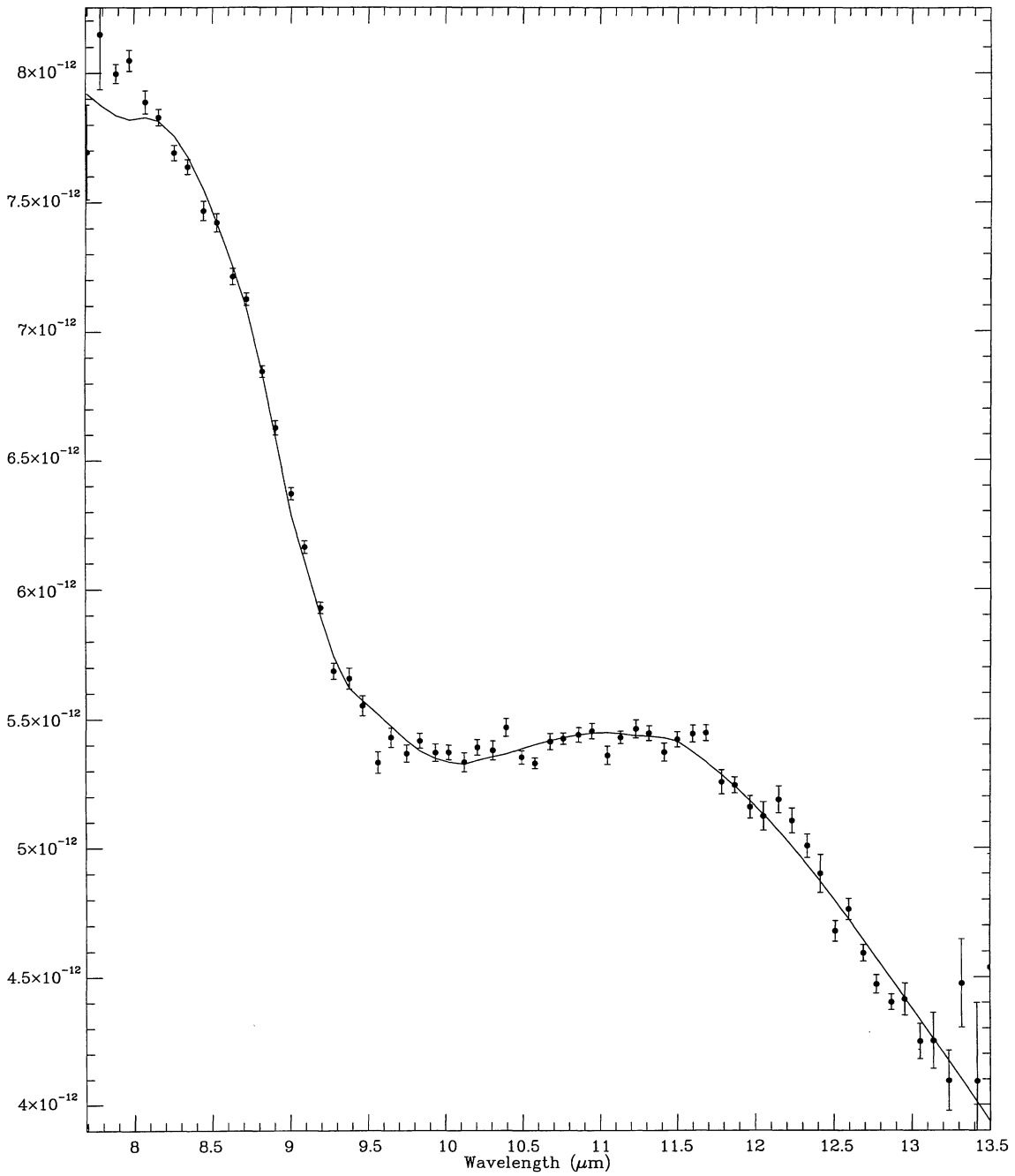

Figure 8. Flux-calibrated spectrum of AFGL 2333, with the best χ^2 fit using self-absorbed silicate.

μm colour temperature. There is an obvious trend, whereby the spectra with the hotter underlying colour temperatures have higher peak to continuum ratios; the linear correlation coefficient is 0.73. This trend is not surprising, since Baron et al. (1987) had already found that the SiC feature tends to get stronger as the temperature of the underlying continuum increases. The sources with underlying continuum temperatures >1200 K cannot be fitted by self-absorbed SiC emission, whereas the sources with $T_{BB}<1200$ K can. The decrease in the peak-to-continuum ratio of the SiC feature with decreasing 8–13 μm colour temperature (i.e., increasing mass-loss rates; Fig. 9a) can be attributed to two effects: (a) for low mass-loss rates there is no dilution of the SiC feature by dust continuum emission originating in the outflow, but as the mass-loss increases the continuum emission produced by an increasingly optically thick dust shell dilutes the SiC emission to an increasing degree; and (b) as the wind mass-loss rate increases (causing the 8–13 μm continuum colour temperature to decrease) the SiC feature itself begins to become optically thick. This self-absorption also reduces the peak-to-continuum ratio of the SiC emission band, and for large enough mass-loss rates the feature ultimately goes into net absorption. The evidence found in the current paper for the major role played by self-absorp-

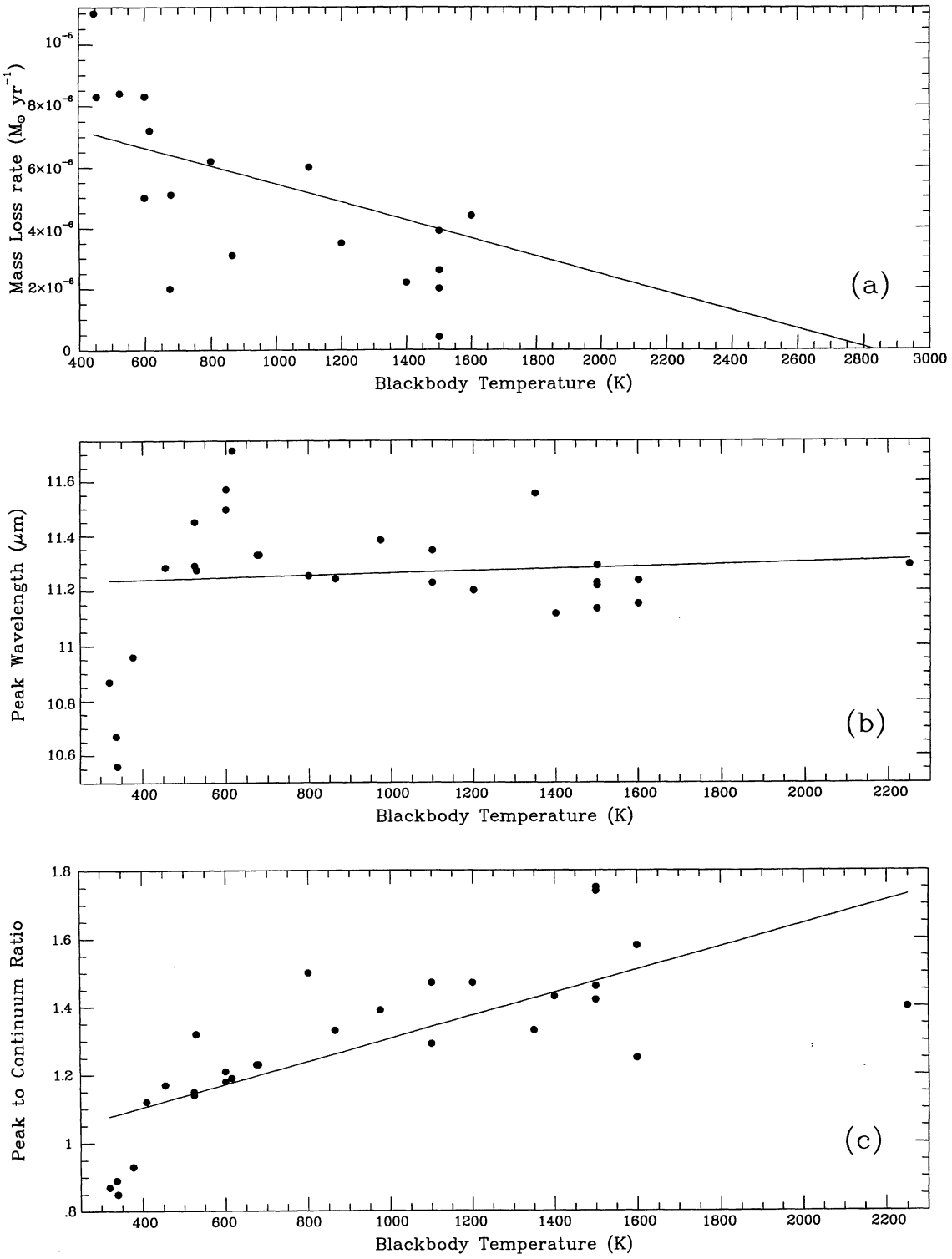

Figure 9. Plots of the 8–13 μm colour temperature versus various parameters: (a) Colour temperature versus the mass-loss rate (from Loup et al. 1993); (b) Colour temperature versus the peak wavelength of the SiC feature; (c) Colour temperature versus the peak to continuum ratio of the SiC feature.

tion in reducing the strength and contrast of the SiC emission feature in the spectra of carbon stars with high mass-loss rates and low 8–13 μm colour temperatures leads us to conclude that it is probably not necessary to invoke the coating of SiC grains by a carbon mantle (e.g. Chan & Kwok 1990; Goebel et al. 1995; Kozasa et al. 1996) in order to explain the observed diminution in the strength of SiC emission from such stars. Radiative transfer modelling is now desirable, in order to ascertain how much SiC is required for the self-absorption to occur. Previous radiative transfer ana-

lyses of the SiC feature have neglected self-absorption and have therefore probably underestimated the quantities of SiC in the outflows.

Chan & Kwok (1990) proposed a scenario for the evolution of SiC dust particles with the evolution of the carbon star that produces them. They suggested that the dust produced when the star has a relatively low mass-loss rate is of the α-SiC variety, since the high densities needed for grain condensation require grain formation to take place close to the star; at the relatively high temperatures that characterize these regions, only α-SiC would be able to condense. As the mass-loss rate increases and the dust shell becomes denser and more optically thick, β-SiC could begin to condense at the lower temperatures characteristic of the regions further out in the circumstellar envelope. Thus β-SiC might be detected, as the envelope could be highly opaque to the inner α-SiC emission. If this model were correct, we should be able to see a difference between the feature shapes and peak wavelengths observed from optically thick and optically thin envelopes. As discussed above, the correlations found in Figs 9(a) and (c) support the view that those carbon stars which have relatively high 8–13 μm colour temperatures have optically thin circumstellar shells and lower mass-loss rates. Likewise those carbon stars with cooler 8–13 μm colour temperatures are likely to have optically thick shells and higher mass-loss rates. However, Fig. 9(b) shows that the peak wavelength of the SiC feature is not correlated with the 8–13 μm colour temperature, whereas if β-SiC was to become more predominant at higher mass-loss rates we would have expected to see a shortward shift of the peak wavelength with decreasing 8–13 μm colour temperature. Inspection of Table 6, in which the sources are listed in order of increasing 8–13 μm colour temperature, shows that, for all the sets of results, there is no tendency for the hotter sources to have α-SiC features and the cooler ones to be better fitted by β-SiC features. In fact, for the 9.5–13.5 μm fitting of the sources with emission features, β-SiC appears as a best fit for only one object, R For, which is probably not a high enough incidence to be significant. Thus, although we have searched hard for the presence of β-SiC grains in our sample of 8–13 μm spectra of carbon stars (motivated by the fact that β-SiC seems to be the dominant type of SiC found in meteorites), we have been unable to find any convincing evidence for β-SiC grains.

Given that our results imply that α-SiC is the predominant form of SiC in carbon star outflows, the apparent predominance of β-SiC grains in meteoritic samples would appear to imply the existence of an unknown conversion mechanism from the α- to the β-form of SiC, perhaps due to irradiation in the ISM or in the protosolar nebula. We note, however, that laboratory mid-infrared absorption spectra of meteoritic SiC samples have yet to be obtained. It has been suggested by T. Bernatowicz (private communication) that the severe twinning of the β-SiC found in meteorites may cause it to produce a spectrum resembling that of α-SiC. Until carbon star and metoritic SiC grains are characterized by the same method, it may be premature to conclude that they are different types. The α-SiC variant appears to be dominant throughout our sample, for the pure emission cases (those with 8–13 μm $T_{BB} > 1200$ K in Table 2), for the self-absorbed emission cases (those with $T_{BB} < 1200$ K in Table 2) and for the four objects exhibiting net absorption in their SiC profiles (Table 8).

ACKNOWLEDGMENTS

We thank Alex Crutchley for help with the observations and flux-calibrations, and Roger Sylvester for advice on the χ^2-fitting routine. We also thank Tom Geballe for providing the spectrum of IRC + 10216, and Ian Crawford and Raman Prinja. Finally, Elric Whittington is thanked for numerous proof readings and constructive criticism. Electronic copies of the spectra can be obtained on request from aks@star.ucl.ac.uk

REFERENCES

Aitken D. K., Roche P. F., 1982, MNRAS, 200, 217
Aitken D. K., Roche P. F., Spenser P. M., Jones B., 1979, ApJ, 233, 925
Alexander C. M. O., 1993, Geochim. Cosmochim. Acta, 57, 2869
Anders E., Zinner E., 1993, Meteoritics, 28, 470
Bagnulo S., Doyle J. G., Griffin I. P., 1995, A&A, 302, 501
Baron Y., de Muizon M., Papoular R., Pégourié B., 1987, A&A, 186, 271
Bernatowicz T., Fraundorf G., Tang M., Anders E., Wopenka B., Zinner E., Fraundorf P., 1987, Nat, 330, 728
Bernatowicz T., Cowsik R., Gibbons P. C., Lodders K., Fegley B., Jr, Amari S., Lewis R. S., 1996, ApJ, 472, 760
Blanco A., Borghesi A., Fonti S., Orofino V., 1994, A&A, 283, 561
Blommaert J. A. D. L., Van Der Veen W. E. C. J., Habing H. J., 1993, A&A, 267, 39
Borghesi A., Bussoletti E., Colangeli L., De Blasi C., 1985, A&A, 153, 1
Chan S. J., Kwok S., 1990, A&A, 237, 354
Claussen M. J., Kleinmann S. G., Joyce R. R., Jura M., 1987, ApJS, 65, 385
Cohen M., 1979, MNRAS, 186, 837
Cohen M., 1984, MNRAS, 206, 137
Cohen M., Davies J. K., 1995, MNRAS, 276, 715
Cohen M., Walker R. G., Barlow M. J., Deacon J. R., 1992a, AJ, 104, 1650
Cohen M., Walker R. G., Witteborn F. C., 1992b, AJ, 104, 2030
David P., Le Squeren A. M., Sivagnanam P., Braz M. A., 1993, A&AS, 98, 245
Evans A., 1994, The Dusty Universe. John Wiley & Son, New York
Forrest W. J., Gillett F. C., Stein W. A., 1975, ApJ, 195, 423
Friedemann C., 1969, Physica, 41, 189
Friedemann G., Gürtler J., Schmidt R., Dorschner J., 1981, Ap&SS, 79, 405
Gilman R. C., 1969, ApJ, 155, L185
Gilra D. P., 1971, Nat, 229, 237
Gilra D. P., 1972, in Code A. D., ed., The Scientific Results from the *Orbiting Astronomical Observatory* (*OAO*). NASA SP-310, p. 295
Gilra D. P., 1973, in Greenberg J. M., van de Hulst H. C., eds, Proc. IAU Symp. 52, Interstellar Dust and Related Topics. Reidel, Dordrecht, p. 517
Gilra D. P., Code A. D., 1971, BAAS, 3, 379
Goebel J. H., Bregman J. D., Witteborn F. C., Taylor B. J., Willner S. P., 1981, ApJ, 246, 455
Goebel J. H., Cheeseman P., Gerbault F., 1995, ApJ, 449, 246
Griffin I. P., 1990, MNRAS, 247, 591
Groenewegen M. A. T., 1995, A&A, 293, 463
Groenewegen M. A. T., 1997, A&A, 317, 503

Groenewegen M. A. T., de Jong T., van der Bliek N. S., Slijkhuis S., Willems F. J., 1992, A&A, 253, 150
Groenewegen M. A. T., Oudmaijer R. D., Goudfrooij P., van den Hoek L. B., van Kerkwijk M. H., 1996a, A&A, 305, 475
Hackwell J. A., 1971, PhD thesis, Univ. College London
Hackwell J. A., 1972, A&A, 21, 239
Hoppe P., Amari S., Zinner E., Ireland T., Lewis R. S., 1994, ApJ, 430, 870
Jones B., Merrill K. M., Puetter R. C., Willner S. P., 1978, AJ, 83, 1437
Jura M., 1986, ApJ, 303, 327
Jura M., 1990, in Tarter J. C., Chang S., Defrees D. J., eds, Carbon in the Galaxy: Studies from Earth and Space. NASA Conf. Publ. 3061, p. 39
Jura M., 1994, ApJ, 434, 713
Jura M., Kleinmann S. G., 1989, ApJ, 341, 359
Jura M., Kleinmann S. G., 1990, ApJ, 364, 663
Jura M., Turner J., Balm S. P., 1997, ApJ, 474, 741
Justtanont K., Barlow M. J., Skinner C. J., Roche P. F., Aitken D. K., Smith C. H., 1996, A&A, 309, 612
Kozasa T., Dorschner J., Henning T., Stognienko R., 1996, A&A, 307, 551
Lebofsky M. J., Rieke G. H., 1977, AJ, 82, 646
Le Squeren A. M., Sivagnanam P., Dennefeld M., David P., 1992, A&A, 254, 133
Lorenz-Martin S., Lefèvre J., 1993, A&A, 280, 567
Lorenz-Martin S., Lefèvre J., 1994, A&A, 291, 831
Loup C., Forveille T., Omont A., Paul J. F., 1993, A&AS, 99, 291
Martin P. G., Rogers C., 1987, ApJ, 322, 374
Mathis J. S., 1990, ARA&A, 28, 37
Merrill K. M., Stein W. A., 1976, PASP, 88, 285
Papoular R., 1988, A&A, 204, 138
Pégourié B., 1988, A&A, 194, 335
Pillinger C. T., Russell S. S., 1993, J. Chem. Soc. Faraday Trans., 89, 2297
Puget J. L., Léger A., Boulanger F., 1985, A&A, 142, L19
Roche P. F., Aitken D. K., 1984, MNRAS, 208, 481
Skinner C. J., Whitmore B., 1988, MNRAS, 234, 79
Stephens J. R., 1980, ApJ, 237, 450
Tang M., Anders E., Hoppe P., Zinner E., 1989, Nat, 339, 351
Taylor A., Jones R. M., 1960, in O'Connor J. R., Smiltens J., eds, Silicon Carbide: A High Temperature Semiconductor. Pergamon Press, Oxford, p. 147
Tielens A. G. G. M., 1990, in Tarter S., Chang S., Defrees D. J., eds, Carbide in the Galaxy: Studies from Earth and Space. NASA Conf. Publ. 3061, p. 59
Treffers R., Cohen M., 1974, ApJ, 188, 545
Virag A., Wopenka B., Amari S., Zinner E., Anders E., Lewis R. S., 1992, Geochim. Cosmochim. Acta, 56, 1715
Volk K., Kwok S., Langill P. P., 1992, ApJ, 391, 285
Volk K., Kwok S., Woodsworth A. W., 1993, ApJ, 402, 292
Whittet D. C. B., Duley W. W., Martin P. G., 1990, MNRAS, 244, 427
Willems F. J., 1988a, A&A, 203, 51
Willems F. J., 1988b, A&A, 203, 65
Willems F. J., de Jong T., 1988, A&A, 196, 173
Woolf N. J., 1973, in Greenberg J. M., van de Hulst H. C., eds, Proc. IAU Symp. 52, Interstellar Dust and Related Topics. Reidel, Dordrecht, p. 485
Wouterloot J. G. A., Brand J., Fiegle K., 1993, A&AS, 98, 589